Structural designs, principles, and applications of thin-walled membrane and plate-type acoustic/elastic metamaterials

Fuyin Ma, Chang Wang, Chongrui Liu, et al.

COLLECTIONS

Paper published as part of the special topic on Acoustic Metamaterials 2021

View Online   Export Citation   CrossMark

ARTICLES YOU MAY BE INTERESTED IN

Acoustic metamaterials
Journal of Applied Physics **129**, 171103 (2021); https://doi.org/10.1063/5.0046878

Control the structure to optimize the performance of sound absorption of acoustic metamaterial: A review
AIP Advances **11**, 060701 (2021); https://doi.org/10.1063/5.0042834

Acoustic metasurface-based perfect absorber with deep subwavelength thickness
Applied Physics Letters **108**, 063502 (2016); https://doi.org/10.1063/1.4941338

Structural designs, principles, and applications of thin-walled membrane and plate-type acoustic/elastic metamaterials

Fuyin Ma,[a] Chang Wang, Chongrui Liu, and Jiu Hui Wu

AFFILIATIONS

School of Mechanical Engineering, Xi'an Jiaotong University, Xi'an 71009, China

Note: This paper is part of the Special Topic on Acoustic Metamaterials 2021.
[a]**Author to whom correspondence should be addressed:** xjmafuyin@xjtu.edu.cn

ABSTRACT

Many advanced physical properties can be realized by using well-designed acoustic metamaterial (AM) structures, which have significant application value in engineering. In particular, thin-walled membrane, plate, and shell-type structures with deep subwavelength thicknesses that can meet light weight requirements have attracted the attention of many researchers and engineers from various specialized fields. This Tutorial systematically introduced the structural design methods, acoustic/elastic wave attenuation and regulation principles, and engineering applications of thin-walled AMs for low-frequency sound insulation, sound absorption, and vibration reduction. In particular, the design methods and sound insulation/absorption properties of thin-walled AMs for realizing narrow-band and broadband sound attenuation were explored. Furthermore, the local resonance bandgap characteristics, quantitative extraction method for the bending wave bandgap, vibration suppression properties, and the design method for local resonance vibration dampers for elastic wave regulation by thin-walled elastic metamaterials were summarized successively. Moreover, other thin-walled AM applications, such as the wavefront steering performance of thin-walled acoustic/elastic metasurfaces, and the active thin-walled AMs, were introduced as well.

I. INTRODUCTION

Noise is a significant environmental pollution factor, severely affecting daily life. It is mainly produced by mechanical vibration and is harmful to most engineering structures and mechanical devices, especially mechanical equipment and precision instruments. Mechanical vibration results in structural fatigue damage or even destruction, affecting the operational performance and durability of the instruments while also affecting the fabrication accuracy of mechanical equipment and the measurement accuracy of devices.[1] Moreover, the noise generated by mechanical vibration significantly reduces the quality of life, endangering the physical and psychological health of humans. For example, the vibration and noise produced by vehicles, such as airplanes and automobiles, affect the comfort of passengers while destroying equipment and even cause safety challenges.[2] In fact, the negative impact of noise on human health is not only limited to the auditory organs but also affects the nervous, cardiovascular, cerebrovascular, and digestive systems. In particular, low-frequency vibration and noise can easily resonate with human organs (such as the heart, lungs, stomach, and nervous system), directly causing damage to the human body and influencing normal physiological functions. Organs resonating with sound waves can cause physical discomforts, such as headaches, nausea, and dizziness. In severe cases, it can cause confusion, breathing difficulties, and even shock, internal organ damage, blood vessel rupture, and death.[3] Therefore, to improve the quality of life and protect physical and mental health, it is essential to control vibration and noise.[4–5] However, effectively manipulating low-frequency vibration and noise via traditional methods is challenging. For example, homogeneous plates are primarily used to attenuate the noise, while their sound insulation capacity obeys the mass density law.[6] Therefore, bulky structures with a large surface density are often required to attenuate low-frequency sound waves effectively.[7–9] It is difficult to satisfy the development requirements for producing light weight, miniaturized, and integrated mechanical equipment and vehicles.

Acoustic metamaterial (AM) represents a new type of artificial subwavelength microstructure (microstructure refers to a smaller structure than the macromechanical component) and belongs to a rapidly developing, specific acoustic wave functional device.[10–15] Since AM can eliminate the constraint relation between the working frequency and the structure size or surface density, it can manipulate sound and elastic waves via well-designed microstructures with deep subwavelength sizes, expanding its application potential to areas such as vibration and noise reduction, super-resolution imaging, and acoustic cloaking.[14–22] Deep subwavelength size indicates that the size of the smallest structure is at least an order of magnitude lower than the relevant wavelength. The initial application target of AM is only to realize low-frequency vibration and noise attenuation.[10] Then, researchers proposed a variety of AM microstructures to realize the negative mass density, negative bulk modulus, simultaneous double-negative effective parameters, total sound reflection, perfect sound absorption, abnormal reflection, subwavelength focusing, and other remarkable acoustic properties. Therefore, researchers have focused on achieving low-frequency noise and vibration reduction using light weight thin-walled structures, such as thin membrane-, plate-, and shell-type structures, to satisfy lightweight requirements. Researchers have mainly focused on realizing strong low-frequency broadband sound reflection via thin membrane- and plate-type structures for sound insulation, which is defined as a way to reduce noise using a structure to isolate the sound source from the audience. The sound insulation performance is generally quantified by the transmission or insertion loss, which is derived from both the reflection and the absorption of the structure. In this Tutorial, the sound insulation structure mainly refers to the reflection-dominated structure rather than the absorption-dominated one. Although the vibration equations of the membrane and the plate are different, and initial tension is required for the membrane to vibrate, the vibration modes of the membrane and the plate are similar. Therefore, they share the same sound insulation mechanism. In 2008, Yang *et al.* proposed a membrane-type AM with a negative mass density that exhibited excellent low-frequency sound insulation performance.[23] Subsequently, using different structural designs, researchers successively designed multi-cell membrane- and plate-type structures, bilayer membrane- and plate-type structures, multi-layer laminated structures, and shell-type structures to improve the broadband sound insulation capability.[16,24–44] In 2012, Mei *et al.* proposed a membrane-type dark AM for sound absorption. This design achieved strong, low-frequency broadband absorption via an ultra-thin structure with a thickness nearly three orders of magnitude lower than the operating wavelength.[45] Then, asymmetric absorption, hybrid absorption, and coherent absorption mechanisms were adopted to successfully design several lightweight subwavelength sound absorbers, achieving perfect sound and broadband absorption.[46–57]

Vibration attenuation represents another vital research consideration and includes the realization of vibration damping, isolation, and absorption through artificial microstructures.[58–80] Plate-type local resonance structures have been presented earlier in terms of light weight, thin-walled metamaterials. The plate structure produces abundant elastic wave vibration modes, allowing the realization of several unique physical properties. During the early stages, researchers mainly investigated the bandgap characteristics of the structure and methods to expand the bandgap bandwidth or increase the number of bandgaps.[58–65] Although the plate-type structure belongs to a two-dimensional periodicity unit, the structure is three-dimensional, relying on several modes in the dispersion curves to generate mode conversion. Therefore, the bending wave bandgap commonly used in engineering applications cannot be extracted directly, necessitating a complex mode analysis.[66–69] Consequently, Ma *et al.* proposed a modal displacement method to extract the bending wave bandgap quantitatively.[70] Vibration suppression can be achieved in different ways via the microstructure design. For example, the vibration damping effect can be achieved in the bandgap frequency range via the locally resonant periodic structure.[71–74] Furthermore, using a transformation optics method, elastic wave metamaterials were designed to guide the propagation direction of the elastic wave, which could be wound around the objective structure to realize vibration damping.[75–80] Moreover, arranging various local resonance units or acoustic black hole structures on the surfaces of the objective structure produced a vibration absorption effect.[81–84] In addition to sound insulation, sound absorption, and vibration attenuation, unique functions, such as the focusing and cloaking of sound and elastic waves, can be realized by manipulating the wavefront of sound and elastic waves.[50,85–92] Of these, the acoustic metasurface is realized using a membrane- or plate-type structure with a resonant cavity or via bilayer membrane-, plate-, or shell-type structures. The elastic wave metasurface is constructed by arranging a structure with a gradient thickness on the thin plate or local resonance units with gradient parameters.

The sizes of metamaterials are often subwavelength, and their physical properties are generally described using homogenization theories. Effective parameters employ the main physical quantities of metamaterials to describe their properties, such as effective mass density, bulk modulus, and shear modulus.[37,93–96] Early research indicated that the structures were mainly passive. Once a structure was designed and manufactured, its parameters were difficult to modify, preventing it from adapting to the changes presented by the external environment. The development of smart materials and structures provided an excellent solution to this problem. Active AMs could be obtained by introducing smart materials into the design scheme. These active metamaterials allowed for a dynamic adjustment of effective parameters through external excitation, significantly broadening the environmental adaptability of vibration and noise reduction structures.[97–109] In general, a variety of light-weight, thin-walled metamaterials can be designed for sound insulation, sound absorption, vibration reduction, and wavefront phase manipulation to achieve the corresponding functions. In addition to narrow-band sound insulation, sound absorption, and vibration reduction, broadband insulation, absorption, and vibration reduction via microstructures can also be realized. However, few engineering applications are currently available for reducing vibration and noise.

This Tutorial is organized according to the logical relationship shown in Fig. 1. First, thin-walled sound insulation AMs, sound absorption AMs, and vibration attenuation EMs are summarized in Secs. II and IV, respectively. Then, other applications, such as thin-walled acoustic/elastic metasurfaces and active AMs/EMs, are
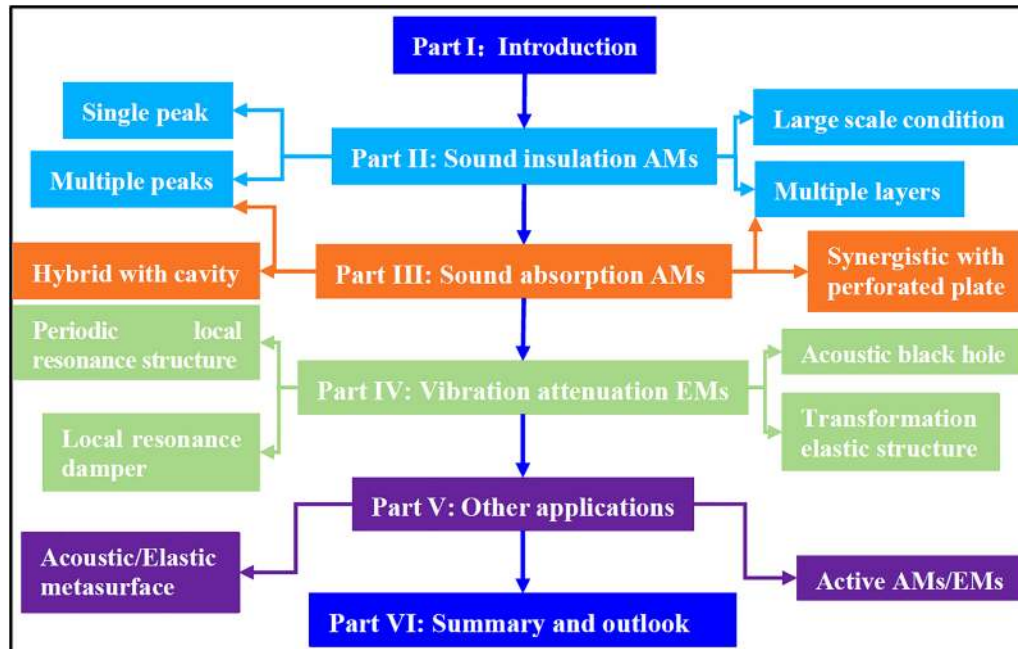
FIG. 1. Schematic of the logical relationship between each part.

introduced in Sec. V. Finally, a brief summary and outlook is presented in Sec. VI.

## II. THIN-WALLED SOUND INSULATION METAMATERIALS

The mechanism of sound insulation through AMs primarily depends on the strong reflection caused by the out-of-phase resonance between the different resonant frequencies of the resonant unit. Due to the advantages of thin-walled membrane- and plate-type structures, such as reduced thickness and low surface density, they are expected to become the preferred choice for low-frequency vibration and noise reduction in practical engineering. Thin plate-type AMs are generally constructed by arranging periodic holes or pillars on a continuous plate, where the thickness of the plate, as well as the size and shape of the holes or pillars, is adjustable. The membrane-type AM differs from the plate-type in that a frame is always used to separate individual cells while one or more masses are arranged on the membrane. Since the rigidity of the membrane is not sufficient to overcome its own gravity, initial tension must be applied to the membrane to support the vibration propagation. Therefore, not only can the unit sizes and shapes of the membrane-type AMs be adjusted but the initial tension can be changed according to the actual requirements. In addition, the resonance frequencies and acoustic characteristics of the unit can be altered by changing the shape, weight, number, and position of the masses.

Extensive research involving membrane- and plate-type structures has been conducted. As early as 1957, Cohen and Handelman studied a circular, fixed-boundary membrane with an attached mass disk, analyzing its vibration characteristics and influence on resonance frequencies.[110] In 1964, Romilly provided an analytical solution to the vibration frequencies and modes of a membrane structure fixed in a rigid cylindrical tube, obtaining its resonance frequencies, anti-resonance frequencies, and transmissions in plane wave incidence conditions.[111] Thin plate structures exhibit similar characteristics to membranes, including bilayer plate-type structures. In 1984, Kriegsmann et al. studied the acoustic scattering behavior of plates and explored the coupling interaction between the fluid field and the membrane, indicating that the fluid domain could play an additional mass role to reduce the resonance frequencies of the membrane.[112] In 1985, Ahluwalia used the matched asymptotic expansion method to analyze the scattering characteristics of monochromatic plane sound waves using thin membranes and plates in long-wavelength conditions.[113] In 1995, Norris et al. studied the acoustic-structure coupling interaction between thin membranes and acoustic waves. The diffraction coefficient variation in conjunction with frequency was comprehensively analyzed, revealing a quasi-resonance phenomenon and exposing its physical mechanism.[114] In 2006, Amabili et al. studied the vibration characteristics of a rectangular thin plate structure with an attached mass disk under simply supported and fixed-boundary conditions, analyzing the influencing factors from the moment of inertia of mass on the vibration frequencies.[115]

The membrane-type AM proposed by Yang et al. in 2008 is shown in Fig. 2(a). The structure consists of a tensioned membrane, a support frame, and an attached mass disk. This unit
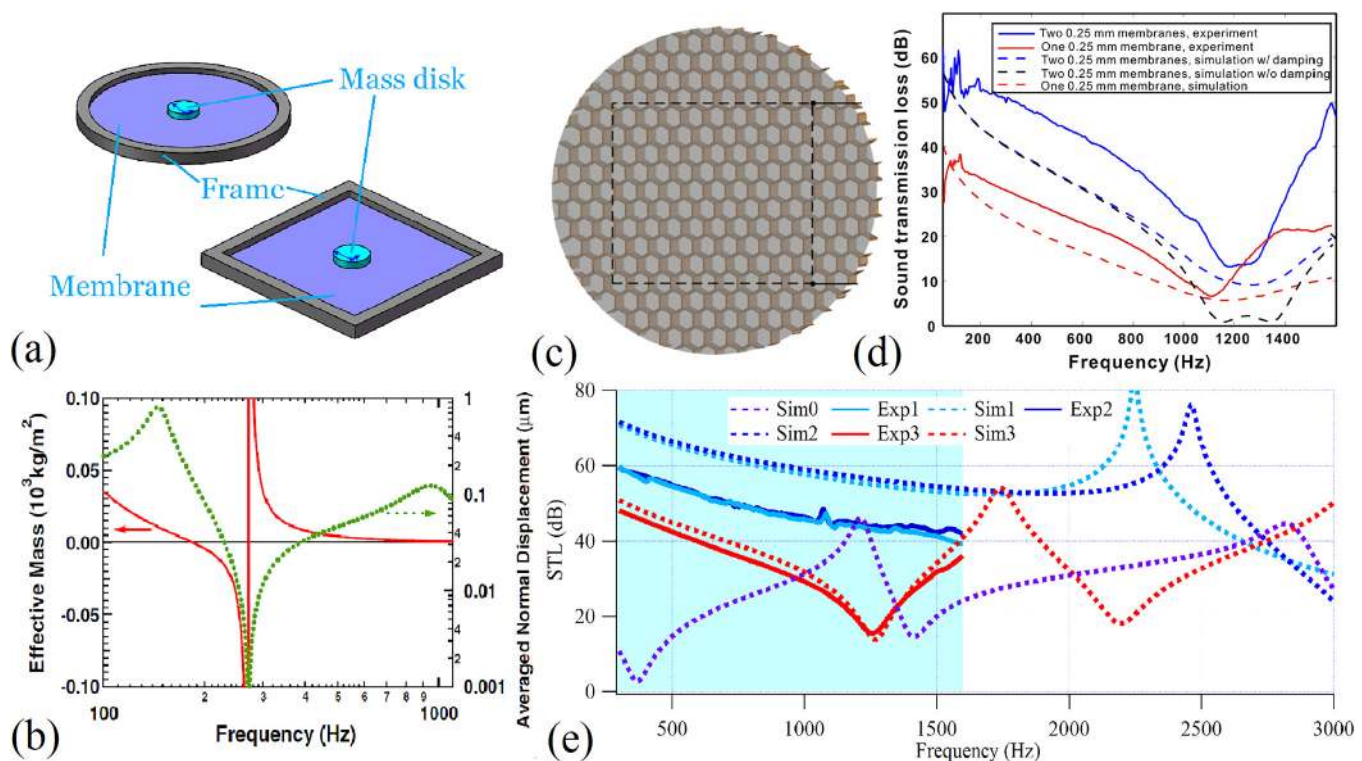
FIG. 2. (a) Single-layer local resonance membrane-type sound insulation unit; (b) effective mass density and averaged out-of-plane displacement of a circular single-layer membrane-type unit.[23] Reproduced with permission from Yang *et al.*, Phys. Rev. Lett. **101**, 204301 (2008). Copyright 2008 The American Physical Society. (c) A membrane-type sound insulation structure with honeycomb frame and (d) the low-frequency sound transmission losses.[30] Reproduced with permission from Sui *et al.*, Appl. Phys. Lett. **106**, 171905 (2015). Copyright 2015 AIP Publishing LLC. (e) The calculation and measurement STL results of plate and shell-type structures with different curvature radii.[32] Reproduced with permission from Ma *et al.*, Sci. Rep. **9**, 8076 (2019). Copyright 2019 Author(s), licensed under a Creative Commons Attribution CC BY 4.0 license.

produced an anti-resonance peak in the frequency range between the first-order and second-order resonance frequencies (transmission peaks), achieving almost total sound reflection at the anti-resonance peak. Figure 2(b) shows that this low-frequency sound reflection is caused by the negative effective mass density of the unit. At the anti-resonance peak, the dynamic mass density tended to be infinite, preventing the sound waves from penetrating the structure. Therefore, this light weight structure with a sub-millimeter thickness could successfully realize outstanding sound insulation in a low-frequency range, providing a new solution for low-frequency noise reduction.[23] Subsequently, Naify *et al.* and Zhang *et al.* investigated the sound insulation and dynamic response characteristics of the membrane-type local resonance metamaterials, indicating that the first sound transmission loss (STL) dip and peak depended heavily on the attaching masses, while the second STL dip was mainly influenced by the membrane properties.[24,25] Increasing or decreasing the weight or surface density of the additional mass caused a shift in the first STL dip to lower or higher frequencies. The frequency position of the STL peak shifted accordingly, while the frequency of the second STL dip remained unchanged. Although the first STL dip and peak positions remained almost unchanged when the surface

density of the membrane increased, the second dip shifted to lower frequencies. Furthermore, the first and second STL dips and peaks moved to higher frequencies with increased membrane tension. This indicated that the positions of the first dip and peak were dominated by the additional mass, while the rigidity of the membrane dominated the position of the second dip. Since the structure attached via a simple mass disk could only produce a few anti-resonant sound insulation peaks in a low-frequency range, while the mass dominated the first dip and peak, researchers proposed a structure with an additional ring-shaped mass, producing multiple sound insulation peaks and improving the low-frequency sound insulation performance.[27,28]

According to the sound insulation theory, the frequency band below the first STL dip belongs to the stiffness control region, while its sound insulation properties are determined by the boundary conditions of the structure.[29] Therefore, by designing a localized frame with higher stiffness to improve the restraining rigidity of the membrane and plate, the sound insulation performance of the structure in the low-frequency range can be significantly improved. For example, Sui *et al.* and Lu *et al.* designed membrane-type structures with honeycomb frames [Fig. 2(c)], achieving excellent low-frequency sound insulation performance, as shown in Fig. 2(d).[30,116]

However, when these structures were expanded from a small-sized sample to a large-scale structure, the resonant frequency of the overall structure decreased, and the frequency of the first STL dip displayed continuous shifts to lower frequencies.[31] Therefore, it is challenging to realize the expected effect in large-scale applications when improving the sound insulation performance in the stiffness control region by increasing the localized stiffness, which is considered the boundary constraint stiffness of the unit—the greater the localized stiffness, the smaller the interaction between the adjacent units. Therefore, Ma *et al.* designed a shell-type metamaterial. In addition to bending rigidity, a shell-type unit also displays membrane rigidity, ensuring that the structure exhibits high stiffness in a wide frequency band.[32] Figure 2(e) shows that the shell-type structure can eliminate the low-frequency cutoff frequency feature in a specific curvature range, achieving strong sound attenuation in a wide frequency range.

Research focuses on enhancing sound attenuation in a broader range since the proposed membrane-type AMs can only improve the sound insulation performance in narrow frequency ranges around the anti-resonance frequencies. In 2010, Yang *et al.* stacked multi-layer membrane-type AMs, as shown in Fig. 3(a), obtaining excellent sound attenuation in a broadband range from 50 to 1500 Hz.[33] Since membrane-type metamaterials take advantage of the low rigidity of the elastic membrane, exceedingly low resonance frequencies and excellent low-frequency sound manipulation could be obtained. However, this kind of structure presents many

limitations, hindering its application in practical engineering. First, due to the low stiffness of the elastic membrane, initial tension is often required to support the vibration propagation. Therefore, its mechanical and acoustic properties are relatively unstable, and a slight change in the tension may cause a frequency deviation of tens or even hundreds of Hz. Consequently, the structure designed according to the predefined frequency band can completely eliminate the expected performance in the narrow design band due to the deviation in the tension once the sample is fabricated, or the original preset STL peak position can change into an STL dip. Second, flexible plastic or rubber materials are often selected to construct the units in membrane-type AMs, which can easily fail even though they are not loaded. Therefore, it is essential to find corresponding alternate materials or structural design solutions. In 2015, Ma *et al.* developed a plate-type AM by increasing the thickness of the membrane and reducing the dependence of the structure on initial tension.

In fact, for sound insulation applications, even a bilayer structure can achieve a good sound attenuation effect. As shown in Fig. 3(b), Ma *et al.* achieved strong sound attenuation using a bilayer plate-type structure with a specific distance between the layers.[50] Bianisotropic acoustic characteristics can be realized using membranes or plates with different parameters to construct an asymmetric bilayer structure. When sound waves irradiate from different sides in such a system, the structure can exhibit strong reflection and absorption characteristics. In addition, laminated multi-layer membrane- and plate-type AMs
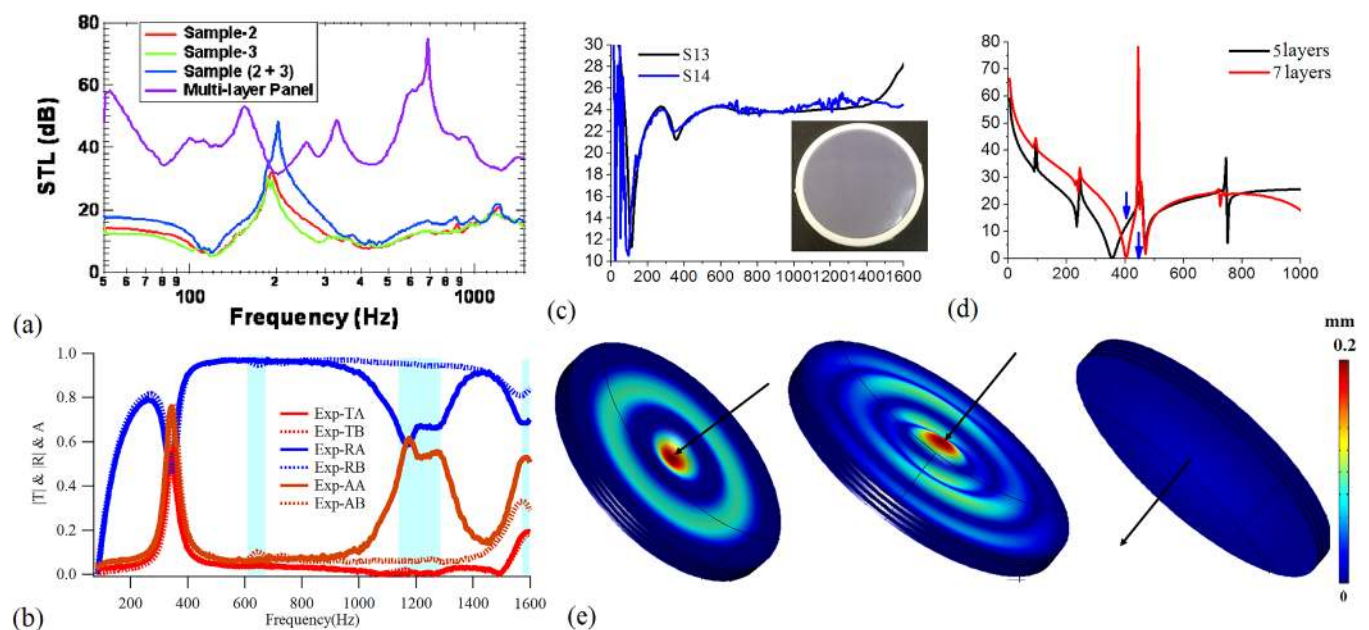

FIG. 3. (a) The STL of the multi-layer membrane-type metamaterials.[33] Reproduced with permission from Yang *et al.*, Appl. Phys. Lett. **96**, 041906 (2010). Copyright 2010 AIP Publishing LLC. (b) The measurement results of sound transmission, reflection, and absorption coefficients of an asymmetric bilayer plate-type metamaterial when sound waves irradiated different sides.[37] Reproduced with permission from Ma *et al.*, J. Appl. Phys. **123**, 035104 (2018). Copyright AIP Publishing LLC. The STL of multi-layer plate-type metamaterials with different layers, (c) measurement sample and results, (d) calculation results, and (e) the displacement profiles of the multi-layer plate-type structure.[34] Reproduced with permission from Ma *et al.*, J. Phys. D: Appl. Phys. **48**, 465305 (2015). Copyright 2015 IOP Publishing.

were designed by introducing a thin air layer between the membrane or plate layers, achieving excellent low-frequency sound insulation performance.[34] These laminated multi-layer structures revealed several novel physical properties, such as a periodical effect, a surface effect, and a saturation effect. Figures 3(c) and 3(d) show that the laminated AM exhibits a distinct saturation effect. When the number of layers reaches a specific value, the STL no longer increases in conjunction with the increased number of periods, demonstrating a saturation effect. Figure 3(e) indicates that the layers of the plates located on the sound incident side produce anti-resonance in the saturation effect frequency range, while the rear layers hardly vibrate. Since most polymer plates are manufactured using extrusion processing, the one-dimensional periodical membrane- and plate-type structures can significantly simplify the mechanical processing procedure, effectively reducing production cost. Therefore, the one-dimensional periodical plate- and membrane-type AMs display excellent application potential for practical engineering and can be extended to large-scale applications.

In addition to the stepwise attenuation of sound waves via laminated structures, multiple sound insulation peaks can be obtained via multi-cell structures consisting of several cells with different parameters, achieving strong broadband sound attenuation. Naify et al. obtained multiple anti-resonance sound insulation peaks using a planar cell array to analyze the influence of insufficient localized frame rigidity on the sound insulation performance.

The results showed a low localized frame rigidity caused a lumped-coupling resonance effect, increasing the bandwidth of the sound insulation frequency range.[39] Zhang et al. also obtained multiple sound insulation peaks by arranging mass disks with different weights on adjacent cells. A lumped element effect (i.e., all elements vibrate as a comprehensive structure) was produced for almost all the locally resonant structures when the localized stiffness was insufficient and failed to completely separate the cells, significantly reducing the wave regulation capability of the structures. Therefore, the lumped element effect denoted a negative factor in locally resonant structures.[40] Ma et al. created positive lumped-coupling resonance behavior by introducing a flexible frame into the plate-type AM, designing a multi-cell lumped-coupling resonance structure, as shown in Fig. 4(a).[41] It is advantageous to adopt a larger planar arrangement in plate-type structures. On the one hand, there is no need for too many supporting structures with sufficiently high localized stiffness to ensure the sound attenuation of the structure. Such supporting structures often contribute most to the surface density, which can then be reduced in the overall structure. On the other hand, by adopting a frame with insufficient localized stiffness to simultaneously act as localized rigidity and additional mass, the coupled bending resonance of the frame and the plate can be realized. Such coupling resonance reduces the anti-resonance frequency of the overall structure, shifting the effective sound insulation frequency band to lower frequency ranges while effectively converting
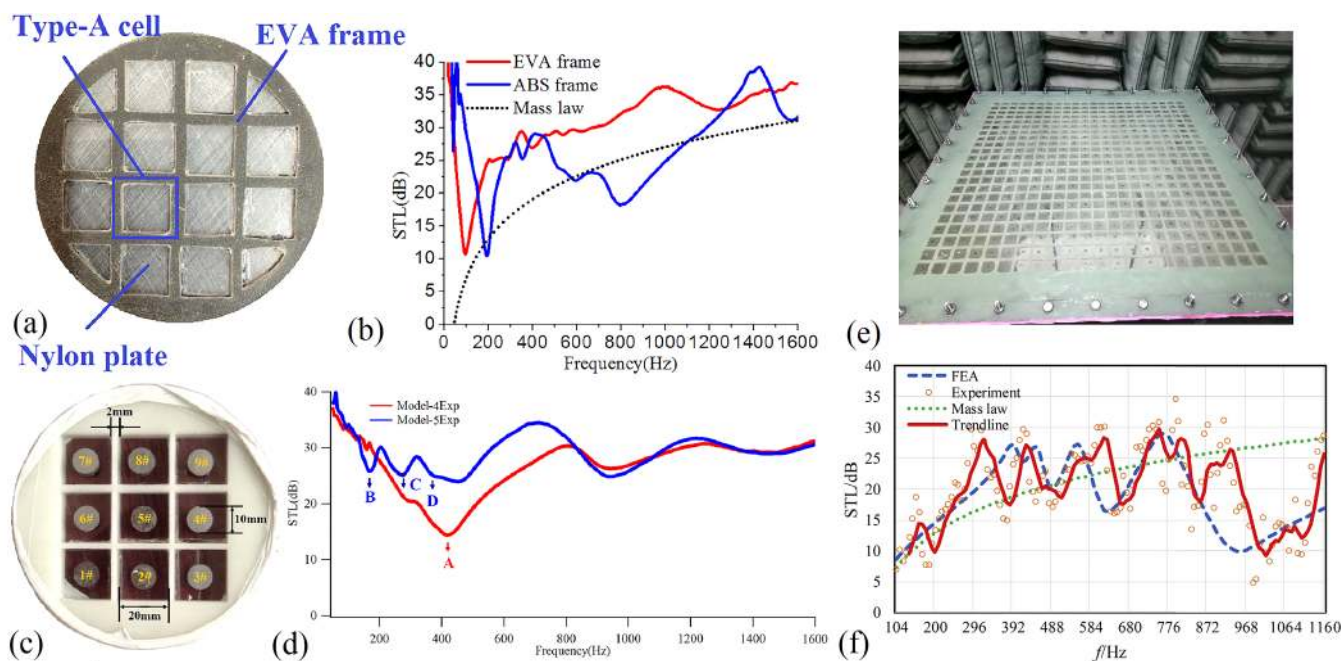
FIG. 4. (a) Multi-cell lumped-coupling plate-type metamaterial with flexible frame and (b) the STL measurement results.[41] Reproduced with permission from Ma et al., J. Appl. Phys. **121**, 015102 (2017). Copyright 2017 AIP Publishing LLC. (c) Plate-type multi-cell synergetic coupling metamaterial with different masses and (d) the STL measurement results.[42] Reproduced with permission from Ma et al., J. Appl. Phys. **122**, 215102 (2017). Copyright 2017 AIP Publishing LLC. (e) Large-scale plate-type multi-cell synergistic coupling metamaterial and (f) the STL measurement results.[43] Reproduced with permission from Wang et al., J. Sound Vib. **459**, 114867 (2019). Copyright 2019 Elsevier.

the lumped resonance effect, which represents a negative factor for low-frequency sound insulation, into a positive factor. As shown in Fig. 4(b), the designed structure exhibits excellent broadband sound insulation performance. When a mass disk is attached to each cell, the average sound insulation can reach a level as high as 32 dB throughout the middle- and low-frequency ranges.

Although significant broadband sound insulation was achieved, as shown in Fig. 4(b), a low sound insulation dip remained, with the lowest STL being only about 10 dB. Ma *et al.* proposed a multi-cell synergetic coupling design method to improve the sound insulation performance in low-frequency ranges, significantly enhancing the sound insulation amplitude at the STL dip. Furthermore, strong broadband sound insulation was realized in a low-frequency range throughout the middle- and low-frequency bands.[42] This structure is illustrated in Fig. 4(c), indicating that the entire structure consisted of multiple cells, each containing an additional mass with a different weight. Figure 4(d) shows the sound insulation measurement results, indicating that the multi-cell synergetic coupling structure produced three distinct sound insulation dips and two peaks due to the use of three groups of additional masses with different weights. The STL curve of the control group exhibited a noticeable dip. The STL amplitudes of the multi-cell synergetic coupling structure always exceeded 24 dB throughout the middle- and low-frequency bands, with an average value of 29.8 dB, indicating excellent broadband sound insulation in the low-frequency range. No synergetic coupling resonance effect was evident between the cells in the control group structure, which produced a pronounced STL dip at an amplitude of only 14 dB. Moreover, the average amplitude in the measured frequency band was significantly lower than the experimental group. A comparison of the STLs of the control and the experimental groups confirmed both experimentally and theoretically that the synergetic coupling resonance effect achieved strong, low-frequency broadband sound attenuation. Notably, units with different parameters can produce multiple sound insulation dips since they are sub-wavelength. Consequently, the sound waves at a specific band show a strong connection only with the unit whose resonance frequency is located around this band, while the transmission properties primarily depend on this unit. If the parameters of each unit are uniform, all units will strongly couple with the incident sound waves, allowing

the maximum transmission, while the STL at the dip can reach an exceedingly low value.

Sound insulation structures are generally used in large-scale conditions during practical applications. Therefore, adapting small-size AMs to large-scale conditions is essential for engineering applications.[16,43,44] Thin-walled AMs applied for reducing low-frequency vibration and noise must ultimately overcome the lumped resonance effect in large-scale application conditions, especially for sound insulation. However, the resonance frequencies of a large-size structure are low, which is unavoidable. Therefore, engineering applications can be realized only via well-designed structures and by eliminating the negative effect of lumped resonance. Wang *et al.* designed a large-scale sound insulation structure with a side length of 0.8 m using the multi-cell synergetic coupling design method, as shown in Fig. 4(e).[43] The measurement and calculation results in Fig. 4(f) indicate that this structure produced multiple sound insulation peaks in the middle- and low-frequency bands, maintaining the sound insulation at a relatively high level in a broader frequency range. Therefore, the multi-cell synergetic coupling design method can be successfully extended to large-scale applications for realizing strong, low-frequency broadband sound insulation. Droz *et al.* improved the sound insulation performance by arranging local resonance units on a large, curved fuselage, providing a basis for promoting the application of metamaterial in actual engineering structures.[117] Langfeldt and Gleine studied the sound insulation properties of metamaterials in elastic supporting boundary conditions, showing that metamaterials exhibit excellent low-frequency sound insulation performance even with insufficient boundary constraints.[118] Table I summarizes the structures, sample thicknesses, and different working bandwidths provided by various representative studies involving sound insulation. It can be concluded that there are four design methods to improve the sound insulation performance: (1) Using membrane and thin plate units with higher frame stiffness or using shell-type units to broaden the frequency band of the stiffness control region; (2) using multi-layer structures to gradually attenuate the sound waves; (3) by employing the strong coupling interaction between the units to increase the number of anti-resonance peaks; and (4) introducing

TABLE I. Comparison of sound insulations.

| Representative works	Structure forms	Total thickness (mm)	Performance	Structure size
Yang *et al.*[23]	Single membrane unit	0.28	Narrow-band insulation	Small size
Sui *et al.*[30]	Membrane unit array	25	Broadband insulation in stiffness control region	
Ma *et al.*[32]	Single shell-type unit	1		
Yang *et al.*[33]	Multi-layers' unit array	60	Broadband insulation with average STL ~40 dB	
Ma *et al.*[34]		2~4	Broadband insulation with average STL ~20 dB	
Ma *et al.*[41]	Strong coupling among units	4	Broadband insulation with average STL ~30 dB	
Naify *et al.*[39]	Weak coupling among gradient parameter	10	Multi-peaks	
Ma *et al.*[42]	units	4	Broadband insulation with average STL ~32 dB	
Wang *et al.*[43]		10	Broadband insulation with average STL ~25 dB	Large size
Ang *et al.*[44]		20	Broadband insulation with average STL ~10 dB	

the multi-cell synergistic coupling interaction between the weak coupling units with gradient parameters to realize continuous sound insulation peaks.

III. THIN-WALLED SOUND ABSORPTION METAMATERIALS

In addition to sound insulation, thin-walled AMs can also achieve low-frequency sound absorption. The sound absorption mechanism via AMs mainly depended on the resonance energy dissipation of the structure, while the absorption peaks are often located at the resonance frequencies. In 2012, Mei et al. proposed a dark membrane-type AM that exhibited strong broadband absorption performance in low-frequency ranges, confirming membrane-type AMs

as a solution for low-frequency noise control.[45] Rectangular membrane units were individually arranged with two symmetrical semi-circular steel sheets as additional masses, separated by a rigid plastic frame, as shown in Fig. 5(a). Under the excitation of sound waves, the two semicircular sheets moved like the wings of a bird, causing sound energy loss. Figure 5(b) shows that a strong broadband sound absorption was achieved when a back cavity was added behind the membrane-type structure. Chen et al. analyzed the sound absorption mechanism of such AMs using the membrane and plate theories, respectively.[46,47] The membrane-type metamaterial exhibited excellent low-frequency sound absorption performance while displaying advantages such as low thickness and surface density. Previous works have indicated that although the membrane-type metamaterial achieved excellent sound absorption, only a few dispersed peaks were
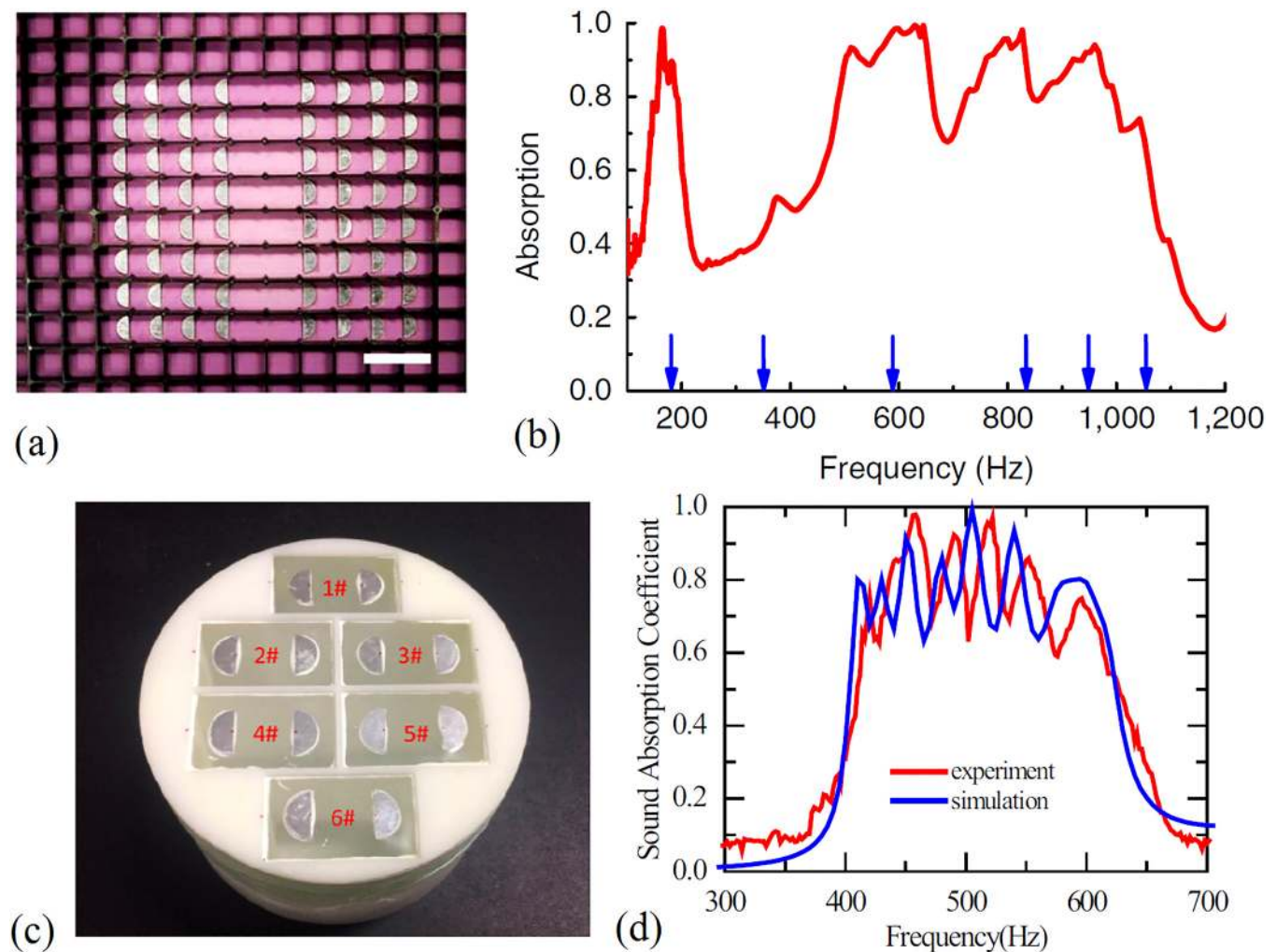

FIG. 5. (a) Membrane-type dark AM and its (b) low-frequency broadband sound absorption results.[45] Reproduced with permission from Mei et al., Nat. Commun. **3**, 756 (2012). Copyright 2012 Macmillan Publishers Limited. (c) Multi-cell synergistic coupling membrane-type broadband sound-absorbing metamaterial and its (d) sound absorption calculation and measurement results.[48] Reproduced with permission from Liu et al., Appl. Acoust. **148**, 1–8 (2019). Copyright 2019 Elsevier.

evident in the low-frequency range. Liu *et al.* adopted a multi-cell, synergetic coupling design method using different mass disks with gradient thicknesses and gradient back cavity depths to facilitate strong broadband sound absorption in low-frequency bands.[48] This metamaterial is shown in Figs. 5(c) and consists of six sound-absorbing cells, each with two semicircular masses. Figure 5(d) indicates that a continuous sound absorption band was obtained in a low-frequency range of 400–600 Hz with a maximum sound absorption coefficient close to 1 and an average sound absorption coefficient of approximately 0.8. The sound absorption frequency band was connected by seven absorption peaks, of which the first six peaks represented the first peak of each unit, while the last peak was caused by the lumped-coupling resonance of the entire membrane-type structure and its sound absorption bandwidth ratio significantly exceeded the other peaks. In theory, this type of structure mainly uses multiple resonance modes produced by the dispersed mass to generate multiple absorption peaks and cooperate with the back cavity to facilitate

energy consumption. Finally, multiple strong sound absorption peaks were connected to obtain super broadband sound absorption. Therefore, asymmetrical mass distribution or a large number of dispersed masses were used to enrich the resonance modes of the unit, while synergetic coupling between the cells with gradient parameters effectively promoted broadband sound absorption.

In theory, the sound absorption characteristics of a structure or material depend on the acoustic impedance, while the best sound absorption effect can be obtained only when its impedance matches that of the sound propagation medium. Therefore, improving the impedance matching properties of the metamaterial and the sound propagation medium enhances the sound absorption performance of the structure, even allowing perfect sound absorption to be achieved. In 2014, Ma *et al.* used an elastic membrane structure with a back cavity to match the impedance with air, successfully obtaining perfect sound absorption in the low-frequency band with a hybrid resonance mechanism. As shown in Fig. 6(a), perfect sound absorption was simultaneously achieved at three
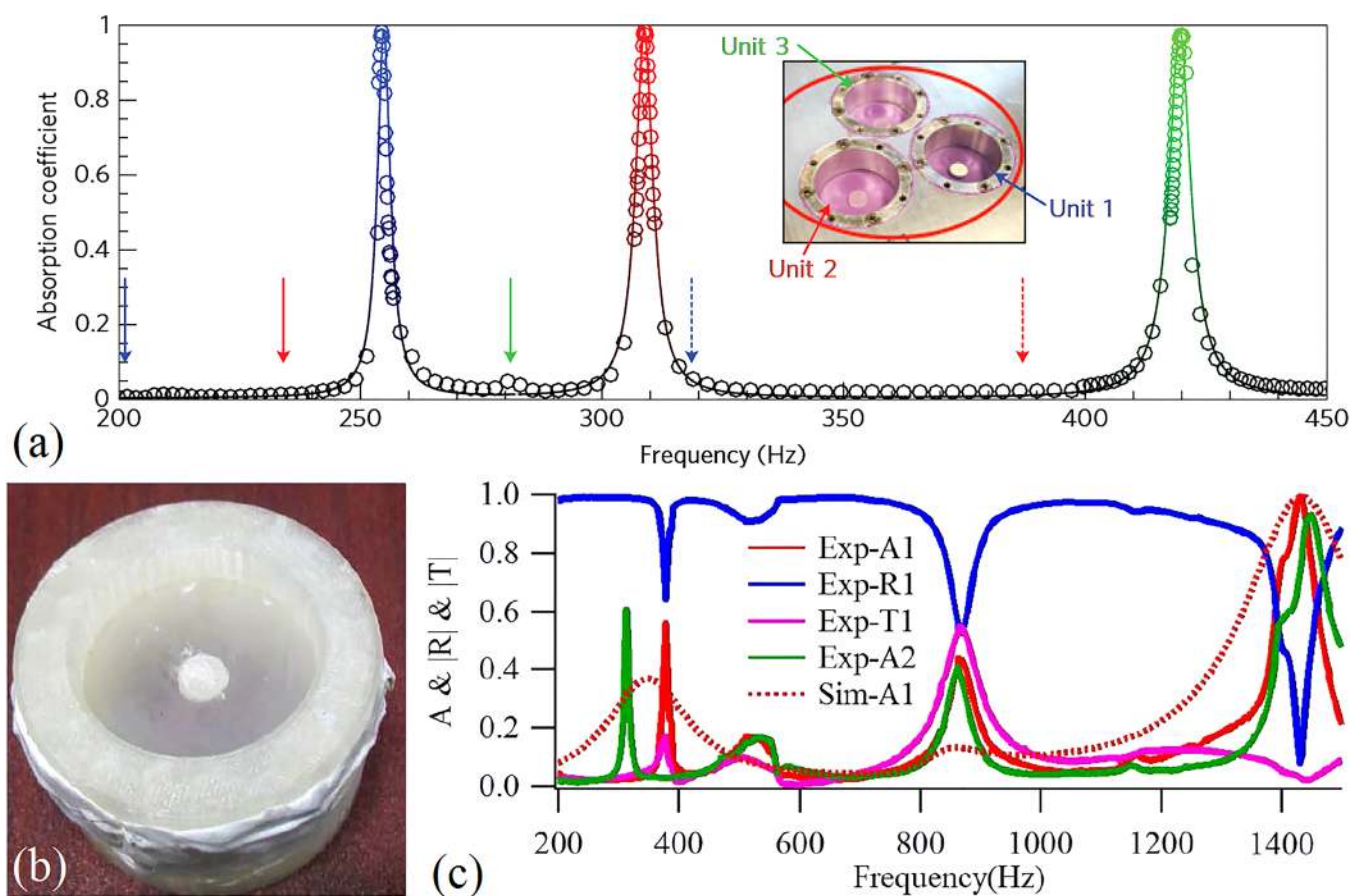

FIG. 6. (a) Membrane-type hybrid resonance sound-absorbing metamaterial and its sound absorption measurement results.[49] Reproduced with permission from Ma *et al.*, Nat. Mater. **13**, 873–878 (2014). Copyright 2014 Macmillan Publishers Limited. (b) Synergistic coupling bilayer plate-type sound-absorbing metamaterial and (c) calculated and measured sound absorption, reflection, and transmission coefficients.[50] Reproduced with permission from Ma *et al.*, Sci. Rep. **8**, 5906 (2018). Copyright 2018 Author(s), licensed under a Creative Commons Attribution CC BY 4.0 license.

frequencies when three different units were used. In this structure, the back cavity was surrounded by several thicker walls to ensure that sound waves were effectively consumed without transmission. However, for applications with stricter lightweight requirements, such as aircraft and vehicles, constructing an air cavity with thicker walls is unacceptable. In fact, the functional decomposition of this membrane-type hybrid resonance-absorbing structure indicates that it can be regarded as a synergetic coupling device composed of three-part components, including a membrane-mass unit that can resonate in-phase with the incident sound wave, the reflective wall of the back cavity, and the sealed air in the back cavity surrounded by the membrane and the reflective walls. This indicates that the total reflection of the back cavity wall is necessary for achieving perfect absorption. Previous studies have shown that light weight membrane- and plate-type AMs can achieve total reflection at anti-resonant frequencies.[23] Therefore, the reflecting back cavity wall can be replaced by a metamaterial unit with anti-resonance properties, and a synergetic coupling bilayer membrane- or plate-type structure can be constructed, as shown in Fig. 6(b).[50] The design procedure of this structure was as follows: (1) a unit was designed that could resonate in-phase with the incident sound

wave as the front plate. (2) A unit displaying strong reflection (often at the anti-resonance frequency) performance was designed as the back plate. (3) These two units were combined with a rigid frame at a specific interval, forming a layer of air at a particular thickness between the layers. (4) The specific order of the resonance frequency was adjusted at the front of the plate-type unit, while the particular order of the anti-resonance frequency at the back of the plate-type unit remained at the same frequency to obtain a composite bilayer plate-type structure. Figure 6(c) shows that the sound absorption coefficient of the structure exceeded 0.99 at the third absorption peak, achieving almost perfect sound absorption.

In addition to membrane-type structures, light weight thin-walled sound absorption metamaterials can also be designed by assembling thin perforated plates or shells with resonant cavities or membrane structures. In 2016, Gai *et al.* proposed a practical structural design method that combined perforated plates with membranes, resulting in excellent sound absorption performance in a broader frequency range.[51,53] Tang *et al.* proposed a composite structure in which a perforated plate covered the perforated resonant cavity, as shown in Fig. 7(a), revealing that the introduction of
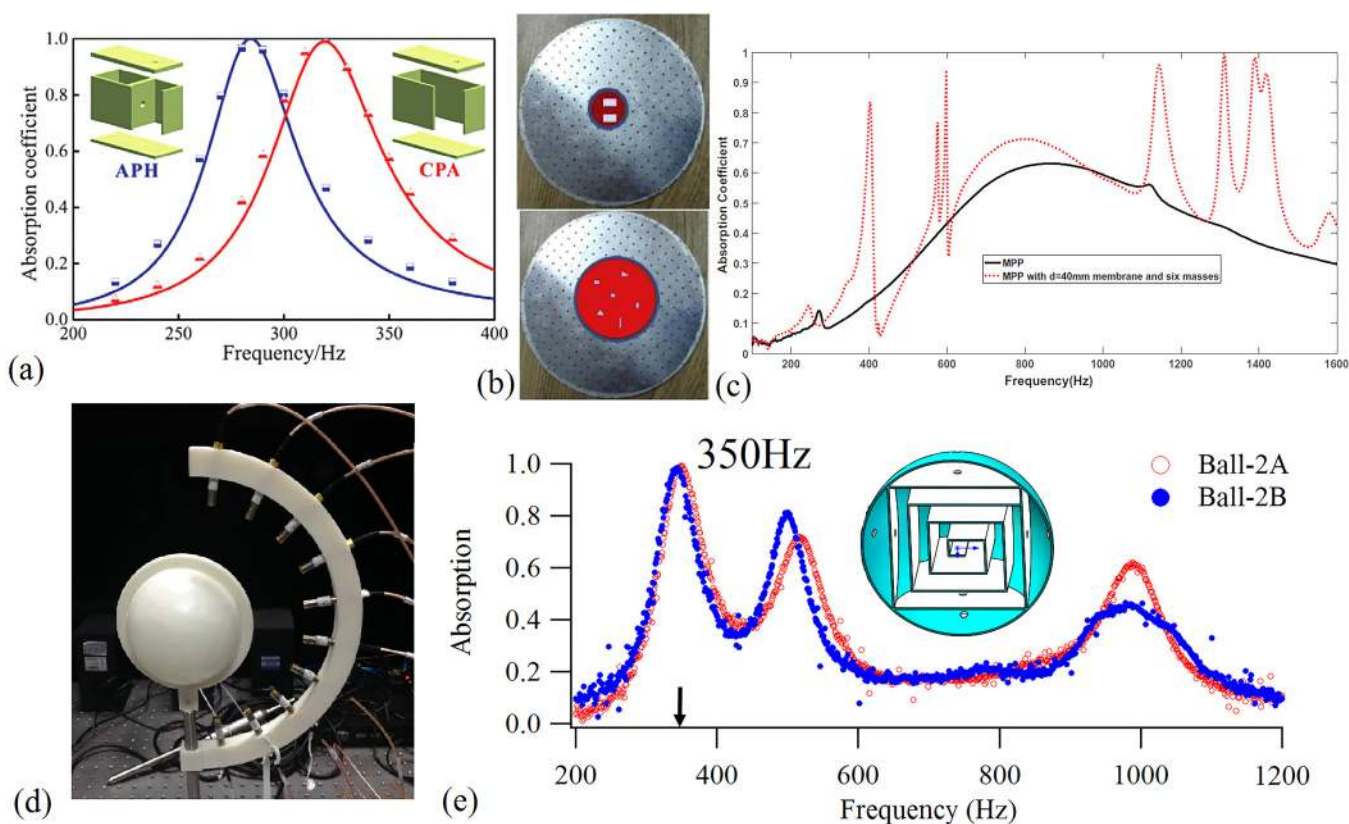
FIG. 7. (a) Perforated plate covering on perforated resonant cavity sound absorption structure and its sound absorption results.[52] Reproduced with permission from Tang *et al.*, Europhys. Lett. **118**, 44002 (2017). Copyright 2017 EPL. (b) Composite sound absorption structure collaborated by perforated plate and membrane, and its (c) sound absorption results.[53] Reproduced with permission from Gai *et al.*, Appl. Acoust. **137**, 98–107 (2018). Copyright 2018 Elsevier. (d) Perforated shell-type sound absorption metamaterial and (e) measured sound absorption results.[56] Reproduced with permission from Ma *et al.*, J. Mater. Chem. C **7**, 5131 (2019). Copyright 2019 Royal Society of Chemistry.

the perforated resonant cavity structure could effectively shift the sound absorption frequency to lower frequencies when the thickness of the structure was maintained as a constant. Although the operational mechanism of the perforated plate structure differed from the resonance membrane- and plate-type structures, in which the plate was treated as a rigid medium, this type of structure also belonged to the thin-walled device and was, therefore, introduced in this Tutorial. In addition, Gai et al. designed a composite structure by combining a micro-perforated plate with a membrane, as shown in Fig. 7(b). As shown in Fig. 7(c), this structure produced multiple additional resonant absorption peaks superimposed over the sound absorption results of the pure perforated plate, effectively improving the sound absorption performance of the structure.[53] Peng et al. proposed a composite structure design method by combining perforated plates with a honeycomb panel. The channel of the honeycomb panel was used as a resonant cavity, while a multi-cell synergetic coupling structure was constructed using different perforation sizes to obtain strong broadband sound absorption.[54] Ma et al. proposed a structural design method that combines perforated shells with labyrinth channels, designing a spherical perforated shell-type sound-absorbing structure, as shown in Fig. 7(d).[56] As shown in Fig. 7(e), perfect sound absorption was achieved in a low-frequency range, while this structure was used as a spherical wave sound sink to achieve sub-diffraction focusing. Maury and Bravo embedded a microcapillary structure in a thin plate to obtain strong broadband sound absorption.[57] Since the sound absorption mechanism of this structure was similar to traditional porous absorption materials, the low-frequency sound absorption effect was poor, while the high-frequency sound absorption performance was superior. Although the membrane-type structure generally displays the highest subwavelength level of all lightweight, thin-walled sound absorption structures, its structural stability is poor, and guaranteeing its durability is difficult, which is not desirable for engineering applications. Therefore, perforated composite sound absorption structures have been vital in achieving excellent broadband sound absorption.[119–124] The structural types, as well as the different operational mechanisms and performance levels outlined by several representative works involving sound absorption, are summarized in Table II. It can be concluded that there are four design methods for thin-walled sound-absorbing metamaterials: (1) using hybrid resonance between thin membrane/plate and air cavity to increase energy loss; (2) using strong coupling interaction between units to increase the number of resonance absorption peaks; (3) by employing the weak coupling interactions between different types of structures to obtain multiple absorption peaks in different frequency bands; and (4) introducing the multi-cell synergistic coupling interaction between the weak coupling units with gradient parameters to realize continuous absorption peaks.

IV. THIN-WALLED ELASTIC METAMATERIALS FOR VIBRATION ATTENUATION

Due to the powerful energy carried by low-frequency vibration, it is difficult to attenuate in a homogeneous medium. Therefore, controlling low-frequency vibration in almost all kinds of mechanical equipment and instruments has continuously presented a significant challenge. Although low-frequency vibration attenuation can be achieved to a certain extent via traditional vibration damping methods, such as dynamic vibration absorbers and vibration isolators, the working principle indicates that their operational frequency bands are often narrow. Therefore, when the actual parameters of the systems or damping components deviate from the design values, the damping effect cannot be achieved, while the vibration performance may also deteriorate. However, the traditional viscoelastic damping material has a weak attenuating effect on vibration at low frequencies. Moreover, adding stiffeners to intensely vibrating areas, or increasing the local thickness of the structure, can also effectively reduce the vibration amplitude in these regions. However, the additional weight is often quite significant, which is not favorable to the light weight design requirements of the structure. Moreover, such methods often substantially affect the original structure, sometimes necessitating changes to the entire design scheme.

In recent years, researchers have proposed local resonance sonics and AMs to enhance low-frequency vibration and noise attenuation since they significantly suppress elastic waves, allowing the flexible control of elastic wave propagation. This kind of artificially designed composite periodic structure can inhibit elastic wave propagation in the bandgap frequency range. The mechanism of vibration attenuation via EMs can be divided into three categories. The first involves locally resonant periodic units, where elastic waves are reflected in the bandgap frequency band and cannot continually propagate. The second type is achieved via a structure exhibiting a non-uniform distribution of the structural parameters

TABLE II. Comparison of sound absorptions.

Representative works	Structure types	Structure forms	Total thickness (mm)	Performance
Mei et al.[45]	Membrane-type unit array	Strong coupling among units	60	Broadband absorption from ~500 to 1100 Hz
Ma et al.[49]	Membrane-type single unit	Hybrid resonance between membrane and cavity	20	Single peak absorption
Ma et al.[50]	Plate-type bilayer single unit	Hybrid resonance among multi-layers	20	
Gai et al.[53]	Synergetic membrane-MPP single unit	Weak coupling among different types of structures	50	Multi-peak absorption
Liu et al.[121]	Synergetic MPP-labyrinth array	Weak coupling among gradient parameter units	72	Broadband absorption from ~380 to 3600 Hz

to guide the elastic wave propagation along a predefined path. The third arranges the local resonance unit as an additional structure on the objective vibration structure to absorb the vibration energy. The bandgap position and width can be adjusted according to the actual low-frequency vibration and noise reduction requirements by paying meticulous attention to the design of the microstructure of the unit and selecting appropriate material for each component. Among the various local resonance microstructures, the plate-type structure is commonly used for constructing two-dimensional periodic structures. Therefore, these structures have received extensive research attention while focusing on phononic crystals and AMs. In 2007, Hsu and Wu examined thin plate structures and obtained the local resonance bandgap of the Lamb wave modes by filling the periodic holes of the thin plate with soft rubber pillars.[58] In 2008, Pennec et al.[59] and Wu et al.[60] independently reported a structure with periodic pillars arranged on a thin plate and analyzed the influence of Lamb wave mode conversion

and the bandgap on the thin plate structures. In this structure, the arrangement of heavier cylinders on the thin plate was equivalent to forming a "solid-version Helmholtz resonator," which could open a vibration bandgap in the range lower than the Bragg bandgap, as shown in Fig. 8(a). Wu et al. constructed a surface-wave waveguide with frequency selectivity functionality using a plate-type pillar structure.[61] Oudich et al. further proposed a bilayer-pillar structure, as shown in Fig. 8(b), and calculated the band structure. As shown in Fig. 8(c), the bilayer-pillar structure could open a bandgap in the range below that of the single-layer pillar structure.[62] Later, they experimentally demonstrated the out-of-plane bending wave bandgap of plate-type structures, as shown in Figs. 8(d)–8(f).[64] Previous studies have shown that by legitimately adjusting the design parameters, this pillar structure can also open multiple bandgaps while even realizing the coexistence of the Bragg scattering and local resonance bandgaps.[63,65] Plate-type metamaterials generally consist of periodic pillars on a thin plate, open periodic holes or slots filled
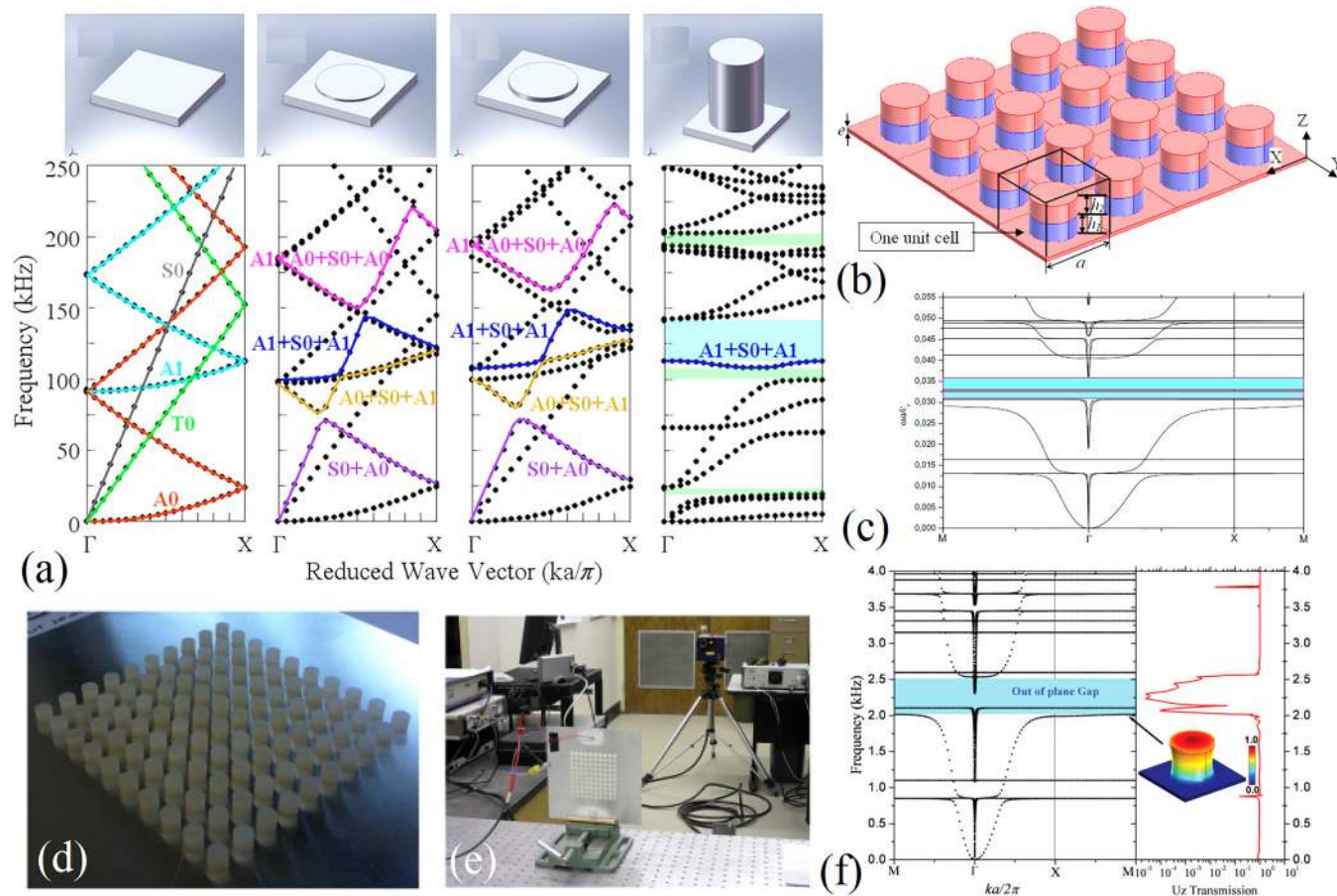

FIG. 8. (a) Plate-type pillar local resonance unit and its band structure.[60] Reproduced with permission from Wu et al., Appl. Phys. Lett. **93**, 111902 (2008). Copyright 2008 AIP Publishing LLC. (b) Plate-type EM array structure with a bilayer-pillar and (c) the band structure of the unit.[62] Reproduced with permission from Oudich et al., New J. Phys. **12**, 083049 (2010). Copyright 2010 IOP Publishing. (d) Periodical plate-type pillar EM array sample, (e) experimental measurement setup, and (f) band structure of the unit.[64] Reproduced with permission from Oudich et al., Phys. Rev. B **84**, 165136 (2011). Copyright 2011 American Physical Society.

with soft materials, and carve different shape beams on plate [Fig. 9(a)]. Early research mainly focused on opening a bandgap, expanding the bandwidth of the band gap, or opening more bandgaps.

Unlike membrane-type structures, plate-type structures can produce abundant surface waves, exhibiting important research value and significant application potential. Since plate-type structures display a higher vibration mode abundance than membrane-type structures, early research has generally focused on their periodicity to analyze their band structures. However, in the case of membrane-type structures, the sound reflection and absorption characteristics are generally explored, with less emphasis on periodicity. Theoretically, the membrane-type structures have similar dynamic characteristics to the plate-type structures. When the rigidity of the membrane reaches a sufficient value to resist its deformation due to gravity, it evolves into a plate-type structure,[29] which exhibits a series of symmetrical and anti-symmetrical Lamb wave modes and shear horizontal wave modes. Figure 8(a) shows

that since these modes exhibit mode conversion on the dispersion curve, their band structure becomes complex, and a detailed analysis of each vibration mode branch is required to determine the bandgaps in different polarization directions. Of these vibration modes, the symmetric Lamb wave mode is an out-of-plane vibration mode, also known as a bending wave mode, playing a dominant role in the vibration along the thickness of the plate and noise radiation. However, the bending wave bandgap cannot be directly and quantitatively determined over extended periods, necessitating a complex mode analysis. In particular, the two-dimensional periodical plate-type local resonance structure often displays three-dimensional geometric characteristics, allowing the bending wave mode propagating along the thickness of the plate to open bandgaps in low-frequency ranges. However, Figs. 9(b)–9(d) indicate other vibration modes existing in the bending wave bandgap frequency range due to the conversion and coupling between modes, as shown in Fig. 9(e).[66–69] Therefore, extracting this kind of bandgap is challenging and requires qualitative mode-shape
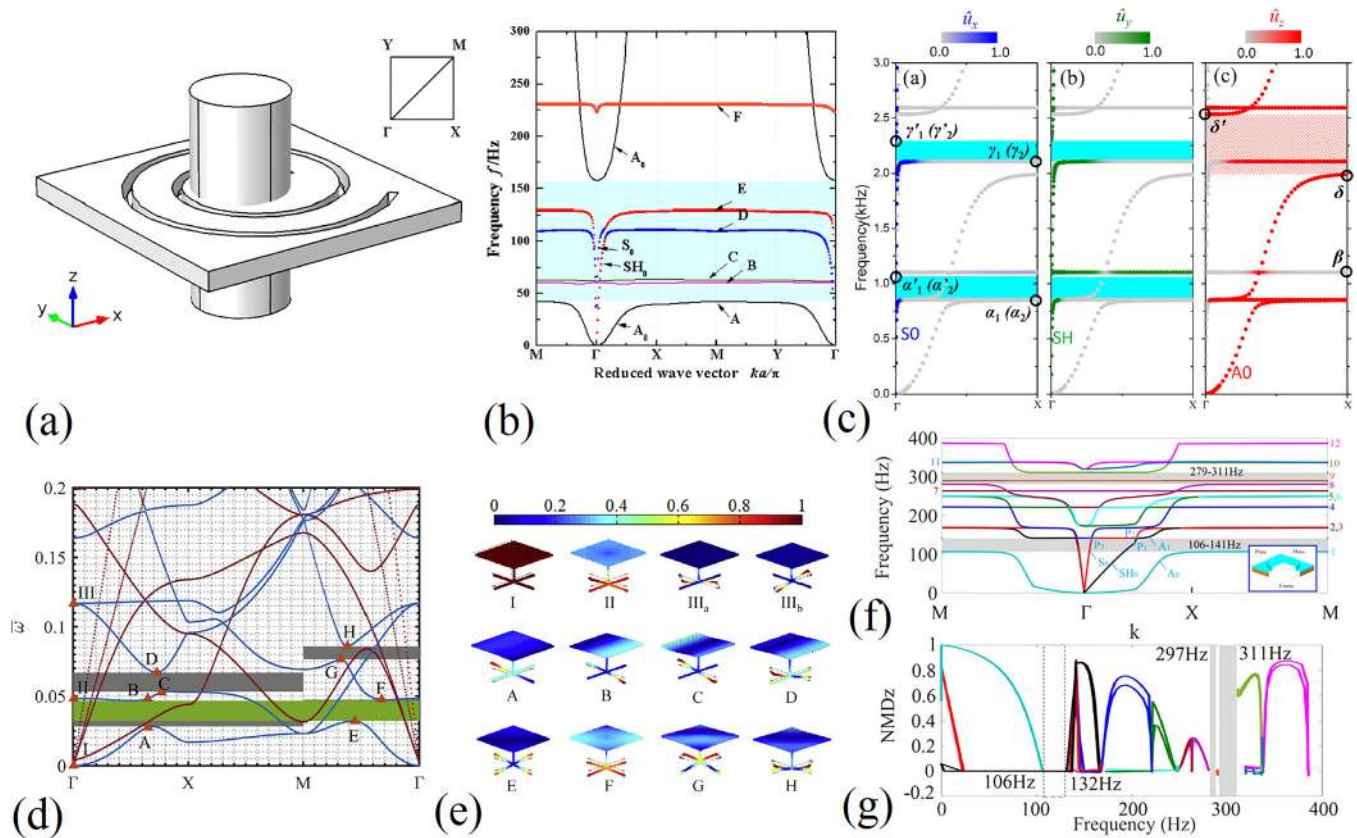

FIG. 9. (a) Local resonance unit with spiral beam engraved on a thin plate and its (b) band structure.[66] Reproduced with permission from Zhang et al., J. Appl. Phys. **113**, 163511 (2013). Copyright 2013 AIP Publishing. (c) Bandgaps with different polarization directions of a plate-type pillar structure.[67] Reproduced with permission from Oudich et al., J. Appl. Phys. **116**, 184504 (2014). Copyright 2014 AIP Publishing LLC. (d) Band structure of a composite plate-beam local resonance unit and its (e) vibration modes.[68] Reproduced with permission from Beli et al., Int. J. Solids Struct. **139–140**, 105–120 (2018). Copyright 2018 Elsevier. (f) The band structure of a plate-type local resonance unit and (g) the modal displacement distribution in the thickness direction of the plate.[70] Reproduced with permission from Ma et al., Appl. Phys. Express **12**, 074004 (2019). Copyright 2019 IOP Publishing.

analysis. Ma *et al.* proposed a modal displacement method for extracting the bending wave bandgap of plate-type AMs. This method replaced the qualitative mode-shape analysis process by quantitatively extracting the statistical averaged modal displacement of the structure. Figure 9(g) shows that the modal displacement in the thickness direction closes to zero at the first bandgap (bending wave bandgap) range shown in Fig. 9(f), realizing the quantitative determination of the bending wave bandgap.

Since the local resonance structure can produce elastic wave bandgaps, it cannot continually spread in the array when the elastic wave propagates in the periodic structure to achieve vibration attenuation. Therefore, vibration damping can be realized if such a periodic structure is arranged in the vibration propagation paths. In 2014, Zhu *et al.* designed a light weight, chiral, locally resonant periodic structure, as shown in Fig. 10(a), achieving elastic wave attenuation in a broadband frequency range.[71] Figure 10(b) indicates that the vibration response amplitude was effectively attenuated in a broadband range of about 150–1000 Hz, compared with the control group. Nouh *et al.* achieved multiple elastic wave

bandgaps in low-frequency ranges by embedding locally resonant periodic units in a thin plate, as shown in Fig. 10(c) obtaining excellent elastic wave attenuation performance.[72] In addition to the locally resonant periodic unit, the EM microstructure can also be designed using acoustic black hole units, as shown in Fig. 10(d), where the vibration energy is concentrated at the tip, after which it is absorbed by damping materials to realize vibration absorption.[73] Therefore, the vibration energy can be transferred from a low frequency to a high frequency to be effectively absorbed, as illustrated by the vibration response results in Fig. 10(e).

In addition to achieving bandgaps, EMs can also guide elastic waves through unique microstructure designs to realize various wave manipulation functions. In 2011, Wu *et al.* designed a double-negative EM with both negative shear and negative bulk moduli, realizing the negative refraction of the elastic waves.[74] Furthermore, they also designed a hybrid elastic unit able to realize several negative effective parameters, obtaining a fluid-like characteristic that could propagate longitudinal waves only in a solid medium.[75] Chang and Hu designed an elastic wave black hole using a
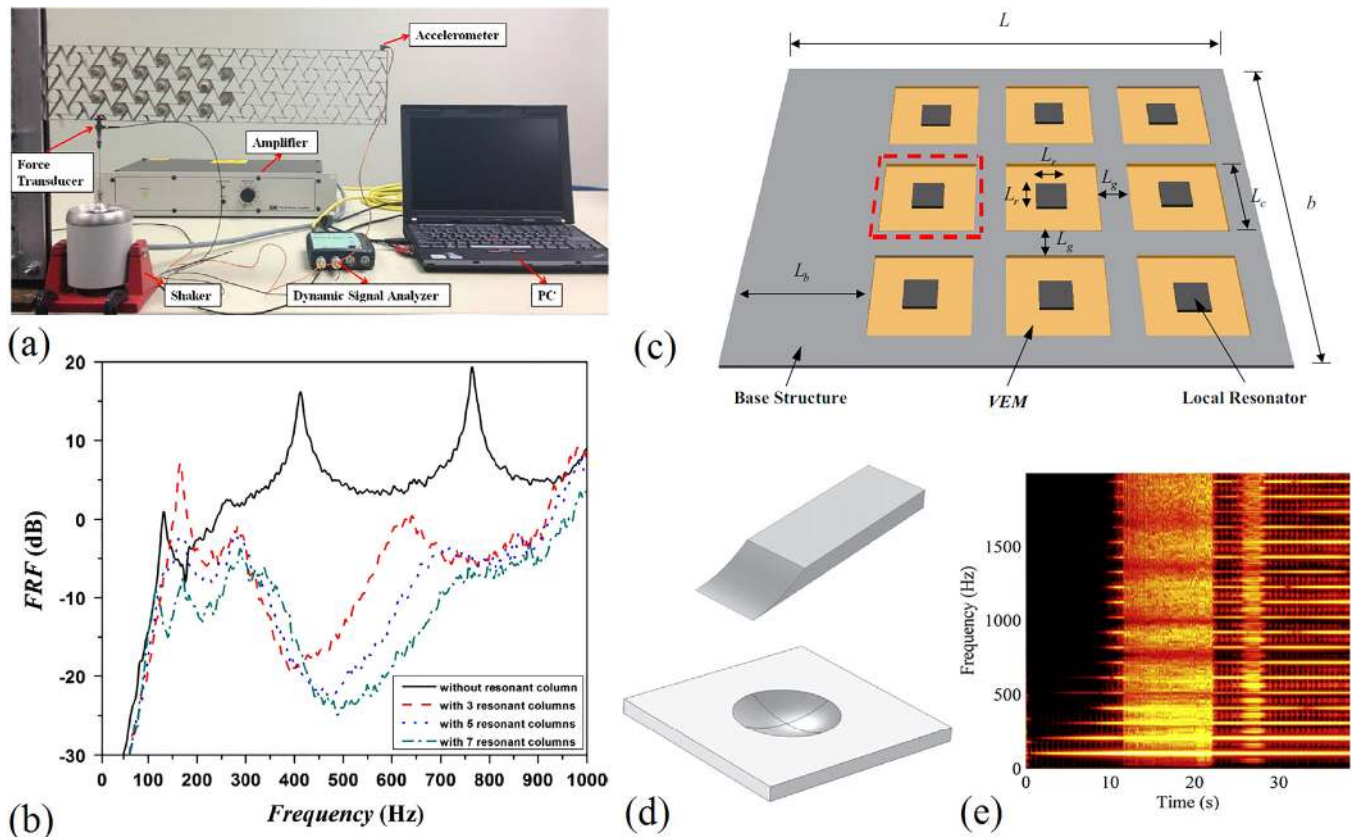

FIG. 10 (a) Experimental setup for vibration transmission measurement of a periodic chiral lattice beam unit and (b) its frequency response function measurement results.[71] Reproduced with permission from Zhu *et al.*, J. Sound Vib. **333**, 2759–2773 (2014). Copyright 2014 Elsevier. (c) Periodic local resonance structure embedded in a thin plate.[72] Reproduced with permission from Nouh *et al.*, J. Sound Vib. **341**, 53–73 (2015). Copyright 2015 Elsevier. (d) One-dimensional and two-dimensional acoustic black hole structures and (e) the vibration response measurement results of an acoustic black hole structure.[73] Reproduced with permission from Pelat *et al.*, J. Sound Vib. **476**, 115316 (2020). Copyright 2020 Elsevier.

transformation method to guide the propagation path of elastic waves to achieve vibration absorption.[76] As shown in Fig. 11(a), microstructures with different effective parameters were arranged at different positions to manipulate the propagation path of elastic waves via coordinate transformation. Figure 11(b) indicates that the elastic waves could propagate along a spiral path, just like a black hole. Zhu et al. also designed a microstructure using the transformation method to guide the propagation path of elastic waves and achieved an elastic wave wormhole effect, as shown in Fig. 11(c).[77] Chen designed periodic grille structures on a single homogenous thin plate via the transformation method to achieve anisotropic AMs that could control flexural waves.[78] Gao et al. designed a single-phase metamaterial plate arrangement using locally resonant periodic units. As illustrated in Fig. 11(d), each unit consisted of four beams, each of which had a mass block at the end.[79] Figure 11(e) shows that each cantilever beam was equivalent to a spring–mass unit, which could be treated as a local resonance composite cell containing multiple spring–mass units. Therefore, it could produce many resonance modes, significantly improving the elastic wave manipulation ability. According to Fig. 11(f), this structure facilitated the flexible manipulation of elastic waves, actualizing special functions, such as the total reflection of sound waves.

Although vibration can be effectively reduced via locally resonant periodic structures, vibration propagation in the primary structure within the bandgap frequency range is challenging. However, these designs adversely change the main structures, limiting the application scope. Therefore, some studies have utilized the local resonance unit as an additional component, which was arranged on the main structure to suppress the vibration.[80–84,125] Peng et al. arranged locally resonant periodic units between the two vibrating plates to effectively reduce the propagation of vibration energy in the plates.[80] Wang et al. used a similar method to effectively reduce the vibration amplitude propagating in the thin plate within the bandgap frequency range of the local resonance unit.[81] Since the local resonance characteristics of EMs do not depend on the periodicity, the vibration energy can be localized in the structure to achieve vibration attenuation even though a single unit is used. Sun et al. designed a membrane-type local resonant unit, as shown in Fig. 12(a), arranging it on the objective structure to achieve vibration absorption. This scheme employed the anti-resonance characteristics of the membrane-type unit, while its operational mechanism was similar to that of the traditional dynamic vibration absorber. The vibration absorption results indicated that this metamaterial vibration absorber was mainly
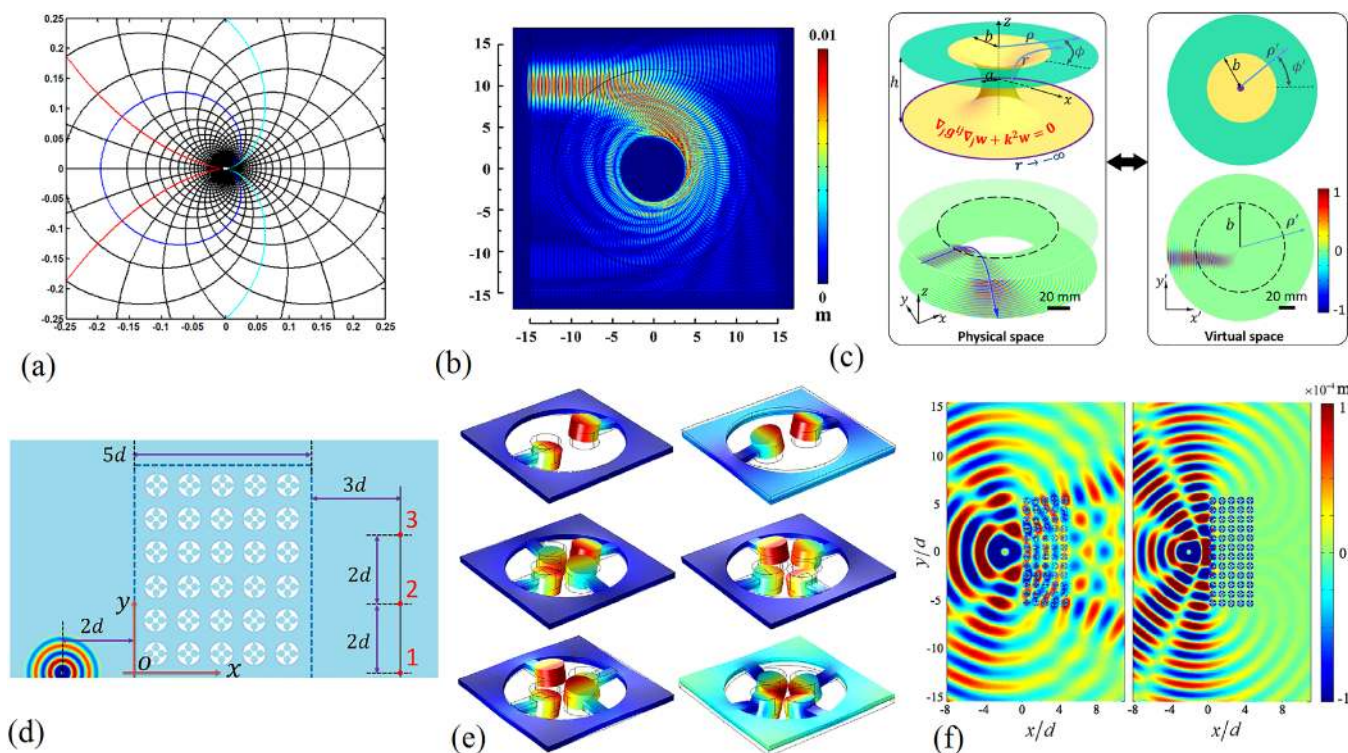
FIG. 11. (a) Elastic wave absorbing structure designed based on the transformation method and (b) the elastic wave propagation effect in the structure.[76] Reproduced with permission from Chang and Hu, Appl. Phys. Lett. **101**, 054102 (2012). Copyright 2012 AIP Publishing LLC. (c) Elastic wave wormhole designed based on the transformation method.[77] Reproduced with permission from Zhu et al., Phys. Rev. Lett. **121**, 234301 (2018). Copyright 2018 American Physical Society. (d) Local resonance composite periodic array, wherein each unit constituted by four beams and each beam with a mass block at the end, (e) the mode shapes of the multi-cell structure, and (f) the elastic wave manipulation effect.[79] Reproduced with permission from Gao et al., J. Sound Vib. **444**, 108–126 (2019). Copyright 2018 Elsevier.
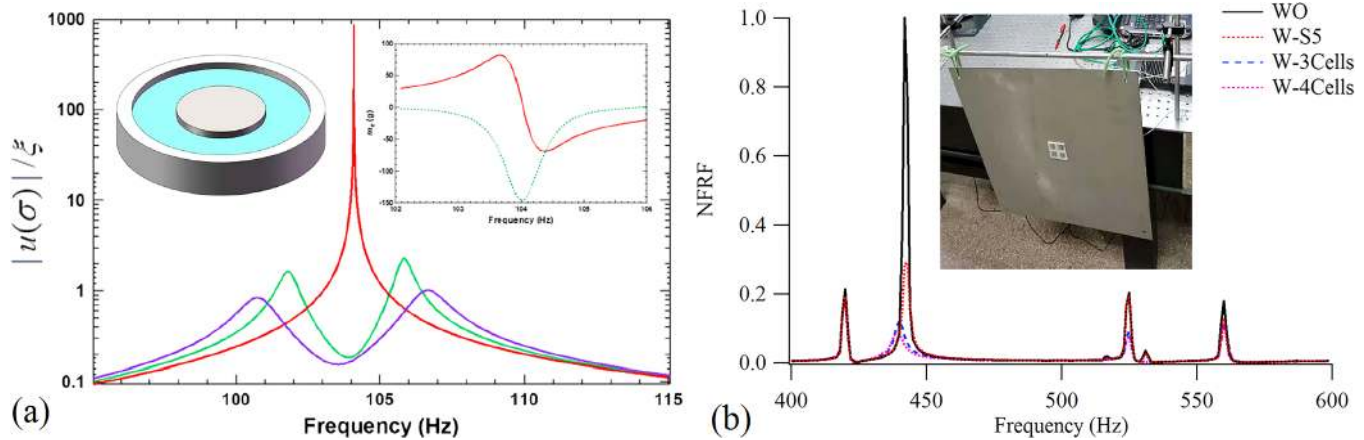
FIG. 12. (a) Membrane-type metamaterial vibration-absorbing unit and vibration suppression effect.[82] Reproduced with permission from Sun *et al.*, AIP Adv. **6**, 085212 (2016). Copyright 2016 AIP Publishing LLC. (b) Ultralight plate-type low-frequency vibration absorption unit and vibration suppression measurement results.[125] Reproduced with permission from Ma *et al.*, J. Phys. D: Appl. Phys. **54**, 055303 (2021). Copyright 2021 IOP Publishing.

operated near the anti-resonance frequency, while two new vibration peaks were produced on both sides of the vibration absorption frequency. Yeh and Harne designed a shell-type reinforced composite structure as a vibration absorption unit arranged on the vibration structure, producing a specific vibration absorption effect.[84] Ma *et al.* designed an ultralight plate-type local resonance vibration absorption unit that differed from that proposed by Sun *et al.* They used the bandgap to determine the vibration absorption frequency range. Figure 12(b) shows that this kind of local resonance vibration absorption unit achieved excellent vibration attenuation. When using four ultralight vibration absorption units, the additional weight was only about 1‰, representing nearly 90% of the vibration amplitude attenuation.[125] In the operating frequency range, the bandwidth and polarization direction of the bandgap were tunable by adjusting the configuration and parameters of the unit cell. This vibration damping method displayed more flexible design properties than the traditional dynamic vibration absorber. Since the configuration of the unit can be easily and flexibly designed according to actual application requirements, it can be used in a wide range of engineering applications, including, but not limited to, aircraft, vehicles, modern industrial equipment, precision instruments, and household appliances. The utilized structure

types, working principles, and performances from representative works involving vibration attenuation are summarized in Table III.

V. OTHER APPLICATIONS

A. Acoustic metasurfaces

To improve the interaction between the waves and the materials, using the smallest possible structures to manipulate the waves, researchers have developed the acoustic metasurface, a type of sub-wavelength wavefront shaping device with a thickness much smaller than the operating wavelength.[14,15,20] Strictly speaking, the metasurface is a functional single-layer structure that can arbitrarily modulate the phase and amplitude of the incident wave and is widely used to replace the bulky phononic crystal structures. In many cases, the performance of these bulky structures may be hindered by the damping loss of the material. Many extraordinary effects, such as abnormal reflection and refraction, can be obtained via these ultra-thin structures. An acoustic or elastic metasurface array covering a 2π phase range is expected to display unconventional acoustic or elastic wave steering capabilities. In addition to sound or elastic wave focusing, the metasurface can also be used to design acoustic or elastic wave cloaks. Therefore, the metasurface

TABLE III. Comparison of vibration attenuations.

Representative works	Structure types	Principle of vibration attenuations	Performance
Pennec *et al.*[59]	Pillar on a plate	Bandgap in a periodic structure	~300 kHz
Hsu[65]	Pillar on a plate	Bandgap in a periodic structure	~20 kHz
Zhang *et al.*[66]	Spiral resonators carved on a plate	Bandgap in a periodic structure	42–150 Hz
Zhu *et al.*[71]	Chiral beam	Bandgap in a periodic structure	~300–600 Hz
Chang and Hu[76]	Transformation structure	Vibration absorption	~800 kHz
Sun *et al.*[82]	Membrane-type resonators	Vibration resonant absorption	~150 Hz
Yeh and Harne[84]	Shell-type resonators	Vibration resonant absorption	~250–325 Hz
Ma *et al.*[125]	Plate-type resonators	Vibration resonant absorption	62–87 Hz

provides an excellent way to manipulate sound or elastic waves via structures with the least substantial thickness and smallest possible size. The metasurface was first developed for electromagnetic waves. Previous studies have shown that metasurfaces with different functions, such as phase discontinuity, abnormal refraction and reflection, and polarization, can be obtained by constructing an interface between two materials. Subsequently, the concept of a metasurface was extended to the fields of acoustic and elastic waves, providing solutions for wavefront shaping in this context.

Several metasurface units, such as labyrinth structures, Helmholtz resonators, and resonant membranes/plates/shells, are commonly used in acoustics. The resonant membrane/plate/shell

structures represent thin-walled structures with excellent subwavelength characteristics that can meet light weight requirements.[50,85,86] In 2016, Zhai et al. proposed a two-dimensional plate-type metasurface unit with a resonant cavity, as shown in Fig. 13(a).[85] A series of metasurface units were arranged on the two hypotenuses of a triangular object. Different units provided various reflection phases according to the height a from the ground, forming an acoustic carpet cloak. When the acoustic cloak was arranged, the sound wave was reflected along the incident direction in a frequency range near the design frequency of 3700 Hz, while no scattered sound field was generated, realizing the acoustic stealth effect. The operating frequency was higher due to a more rigid plate-type structure.
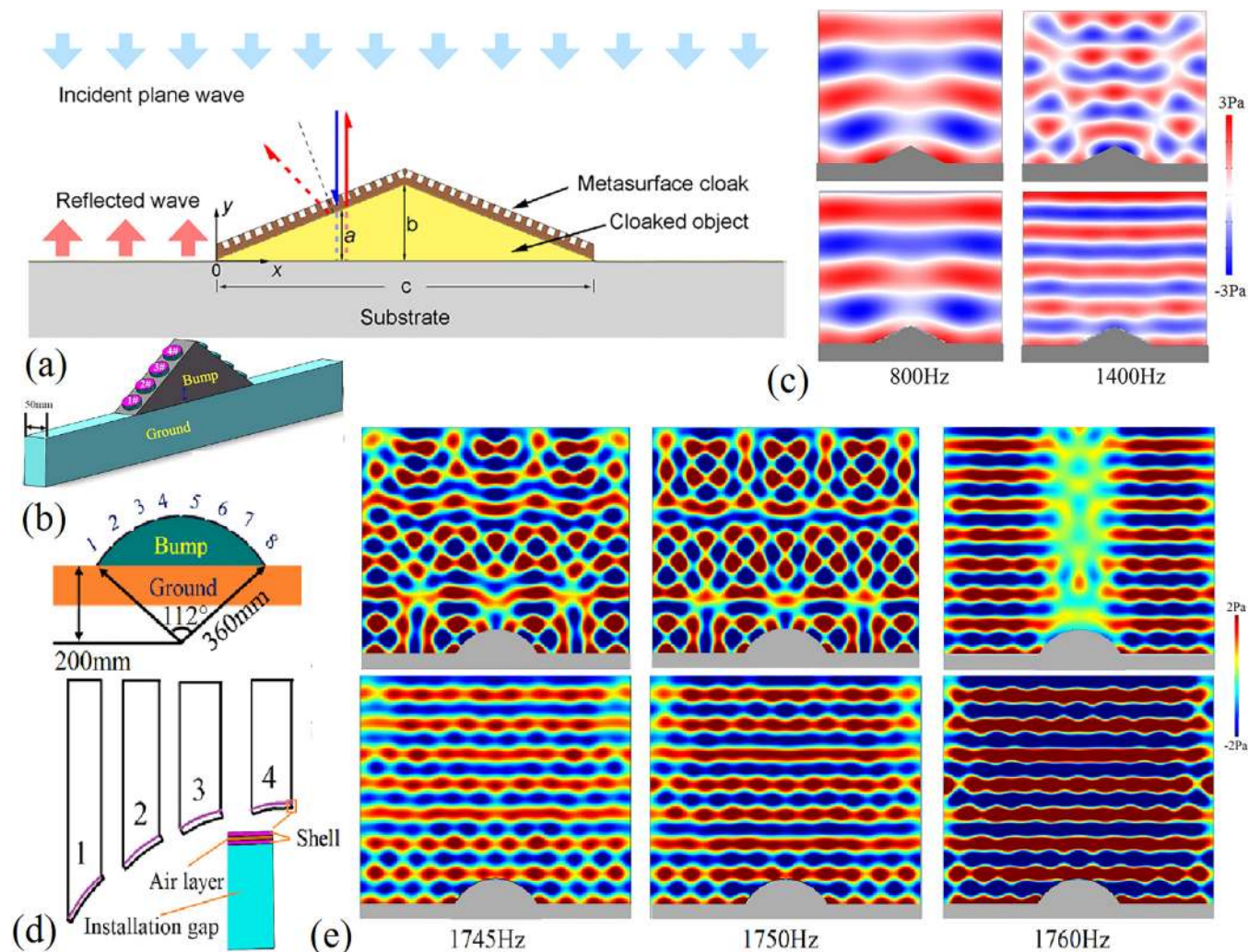
FIG. 13. (a) Two-dimensional plate-type metasurface acoustic cloak structure.[85] Reproduced with permission from Zhai et al., J. Phys. D: Appl. Phys. **49**, 225302 (2016). Copyright 2016 IOP Publishing. (b) Three-dimensional bilayer plate-type metasurface acoustic cloak structure and (c) the acoustic stealth effect of the two-dimensional bilayer acoustic cloak.[50] Reproduced with permission from Ma et al., Sci. Rep. **8**, 5906 (2018). Copyright 2018 Author(s), licensed under a Creative Commons Attribution CC BY 4.0 license. (d) The unit of the bilayer shell-type arbitrary arc-shaped cloak structure and (e) the stealth effect of the shell-type arc-shaped carpet cloak.[32] Reproduced with permission from Ma et al., Sci. Rep. **9**, 8076 (2019). Copyright 2019 Author(s), licensed under a Creative Commons Attribution CC BY 4.0 license.

Moreover, the simplified conditions of two-dimensional structures are difficult to satisfy in practical applications, especially for thin-walled structures since their acoustic properties change after being extended to three-dimensional conditions. Therefore, Ma *et al.* proposed a three-dimensional bilayer plate-type acoustic metasurface, as shown in Fig. 13(b). This structure could achieve a continuous phase shift at lower frequencies.[50] With a triangular structure as the object, four bilayer plate-type acoustic metasurface structures were arranged on both hypotenuses to form an acoustic carpet cloak, obtaining a narrow-band acoustic stealth effect with a bandwidth of about 50 Hz around the design frequency. Furthermore, they created a two-dimensional bilayer plate-type acoustic cover-layer using the acoustic metasurface design method with a gradient phase shift, revealing an excellent ability to retain broadband plane waves, as shown in Fig. 13(c). Since the function of the metasurface unit is to achieve continuous reflection phase adjustment, there is no need to maintain a large enough gap between the plate layers for sound absorption. Therefore, the thickness of this acoustic cloak can be reduced to the sub-millimeter level.[86] The reduction of the interlayer distance is useful for improving the reflection coefficient of the unit, enhancing the acoustic stealth performance of the cloak.

Of the numerous types of acoustic cloaks, the thickness of the carpet cloak is small enough, presenting excellent application potential. However, the cells used in carpet cloaks commonly belong to planar structures. In 2017, Wang *et al.* proposed a two-dimensional spiral acoustic metasurface structure, in which a large number of units were arranged on the surface of a curved object to be invisible, forming a curved acoustic carpet cloak.[87] However, the connection surface between the metasurface units and the objective structure was not curved. Therefore, the expected performance for objects with arbitrary shapes could only be partially realized via the approximation of an arc curve by a straight line when the curvature of the cell coverage area was small. Moreover, when the invisible object exhibited a significant curvature, it was impossible to obtain a carpet-like stealth cloak that could completely fit the surface. Consequently, Ma *et al.* developed a bilayer plate-type acoustic metasurface in a thin-shell structure system, proposing a shell-type acoustic metasurface, as shown in Fig. 13(d).[52] This thin-shell unit could achieve continuous reflection phase shifts covering a 2π range, satisfying the acoustic cloak design requirements. Figure 13(e) shows that this shell-type cloak produced the acoustic stealth effect in a specific frequency range. In addition, considering that the phase compensation of a complex arc-shaped shell-type structure could not be accurately calculated via theoretical relationships, they also proposed an engineered isophase design method for delicate phase compensation adjustments. Therefore, since the shell-type structure can be designed according to the surface profile of the invisible object, an invisible carpet cloak that completely matches the surface can be obtained, presenting the possibility of designing an arbitrarily shaped carpet stealth cloak.

B. Elastic metasurfaces

The elastic metasurface can consist of differently sized pillars, convex bodies with different heights, or resonant units with different inherent frequencies, while elastic wave manipulation can be achieved by adjusting the impedance or phase of the wavefronts.

In 2015, Colombi designed an elastic wave cloak using a series of local resonance units.[88] This cloak consisted of several pillars with gradient heights, facilitating the elastic wave stealth effect in a specific frequency range. Lee and Kim added silicon pillars to a copper plate containing several drilled holes with gradient diameters to design an elastic cloak, as shown in Fig. 14(a).[89] Figure 14(b) shows that the hole in the plate did not cause obvious elastic wave scattering, thus resulting in an excellent elastic wave stealth effect. Xu *et al.* designed a non-resonant single-phase meta-slab with subunits of graded thicknesses, as shown in Fig. 14(c). Here, several convex bodies at different heights were arranged on both sides of the plate, realizing transmission phase manipulation. As shown in Fig. 14(d), this structure produced elastic wave phase shifts covering a 2π range. Furthermore, a plate sample was fabricated that arranged convex bodies at gradient heights, while the distribution of the elastic wave fields on the plate was measured using a laser vibrometer. Figure 14(e) indicates that the elastic waves were deflected in the expected direction. Yuan *et al.* proposed a switchable multi-functional locally resonant metasurface unit, as shown in Fig. 14(f).[91] Various advanced elastic wave manipulation functions such as elastic wave directional deflection, focusing, and beam bending were realized via the array structure of this unit, as shown in Fig. 14(g). Zhang *et al.* designed a 3D printed elastic metasurface, as shown in Fig. 14(h).[92] This metasurface unit consisted of folded beams, in which the phase shift of the wavefront could be adjusted via the different beam heights. The elastic wave-focusing effect shown in Fig. 14(i) was then realized via the gradient parameter structure. Generally speaking, the wavefront manipulation function of the acoustic metasurface can also be realized via the elastic metasurface in the elastic wave system using appropriate structural design. However, the experimental characterization of elastic wave manipulation requires the use of expensive laser vibrometers. Therefore, fewer related works are available than those involving acoustic waves.

C. Actively tunable acoustic metamaterials

Although these functional microstructures can achieve low-frequency sound insulation, sound absorption, vibration reduction, sound focusing, and acoustic stealth functionality, most of the AMs mentioned above are passive. Once the structure was designed and manufactured, its parameters were difficult to modify and it could not adapt to changes presented by the external environment. The development of smart materials and structures provided an excellent solution for this problem. Active AMs can be designed by introducing smart materials into structural design. In active metamaterials, the effective parameters can be dynamically adjusted via external excitation, realizing the tunable design of acoustic performance and elastic wave manipulation. Smart materials and structures that exhibit actively tunable vibration and acoustic properties can be roughly divided into four categories.[97,98] The first uses piezoelectric materials to actively regulate structural stiffness.[99,100] The second regulates the structural parameters by applying an external magnetic field.[101,102] The third employs mechanical devices to regulate the structural parameters or the shifts in the operational states.[103–105] Finally, the fourth regulates the structural parameters by applying an electric field.[106–109] These four implementation methods are
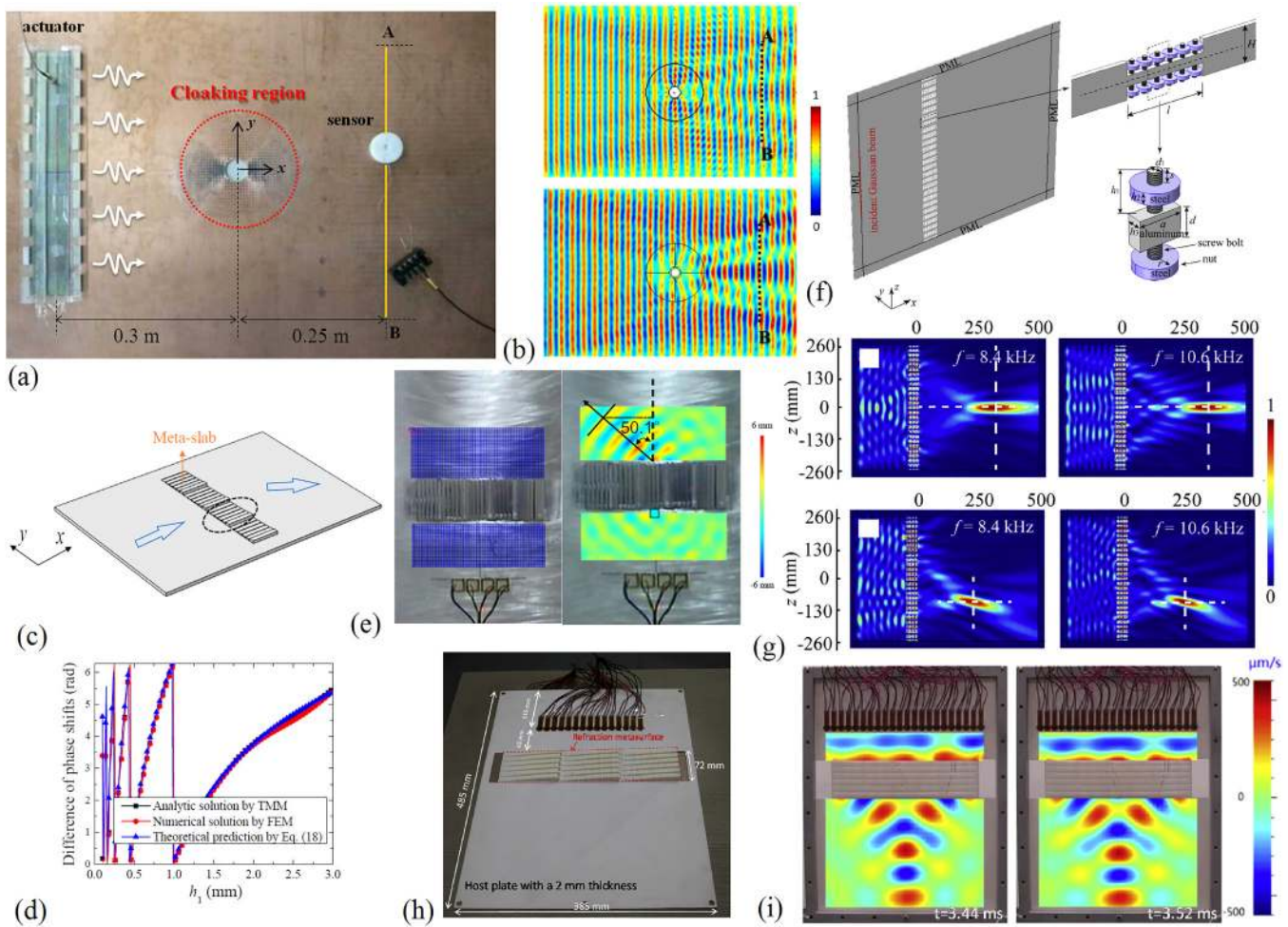
FIG. 14. (a) The perforated plate-type structure of the elastic wave cloak with embedded cylindrical units and its (b) elastic wave stealth effect.[89] Reproduced with permission from Lee and Kim, Sci. Rep. **6**, 20731 (2016). Copyright 2016 Author(s), licensed under a Creative Commons Attribution CC BY 4.0 license. (c) Non-resonant elastic wave metasurface constituted by units with gradient heights, (d) phase profiles of the used units, and (e) experimental setup and the elastic wave manipulation effect.[90] Reproduced with permission from Xu et al., J. Sound Vib. **454**, 51–62 (2019). Copyright 2019 Elsevier. (f) A thin plate arranged with local resonance elastic metasurface units and details of the units and (g) elastic wave-focusing effect.[91] Reproduced with permission from Yuan et al., J. Sound Vib. **470**, 115168 (2020). Copyright 2020 Elsevier. (h) Experimental setup of a plate structure with a folded elastic metasurface and (i) elastic wave-focusing effect at different moments.[92] Reproduced with permission from Zhang et al., J. Sound Vib. **481**, 115440 (2020). Copyright 2020 Elsevier.

suitable for designing conventional smart structures as well as active AMs.[126–128]

In terms of thin-walled metamaterials, the earliest proposed active metamaterial was piezoelectric, as shown in Fig. 15(a).[99] The stiffness of the piezoelectric plate changed when exposed to an applied voltage, actively adjusting the working frequency. Single-layer and bilayer piezoelectric plate-type units were designed, realizing a tunable, effective mass density, and bulk modulus in a frequency range of 2000–3000 Hz. Zhang et al. prepared a membrane-type smart metamaterial by arranging piezoelectric plates on the surface of an elastic membrane, realizing tunable multi-mode sound insulation.[100] Although the tunable frequency

band of the active metamaterial based on piezoelectric materials was relatively wide, the material was expensive and highly rigid, significantly limiting their use in practical applications. Another way to realize the active metamaterial design is to introduce an external magnetic field into the structural design to allow for the dynamic adjustment of structural stiffness. Chen et al. designed an active plate-type magnetic metamaterial, in which the rigidity of the plate changed when exposed to the magnetic field, realizing the active tunability of the resonance frequency.[101] Zhao et al. designed an active membrane-type magnetic metamaterial, as illustrated in Fig. 15(b), where a magnetic mass was arranged on a plate. As shown in Fig. 15(c), the membrane will be inwardly concave under
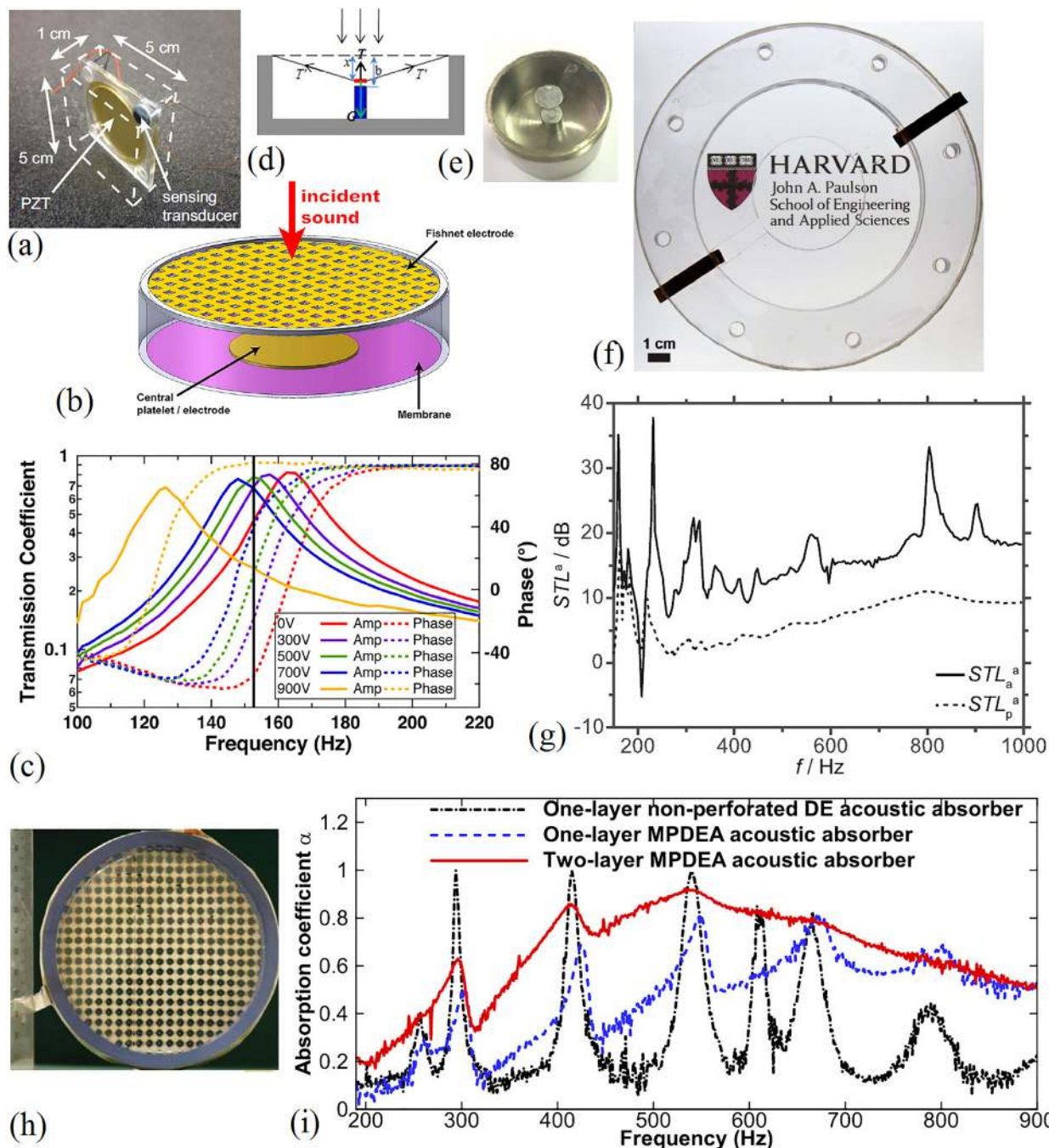
FIG. 15. (a) Active piezoelectric plate-type sound insulation unit.[97] Reproduced with permission from Kumar and Lee, Int. J. Appl. Mech. **11**, 1950081 (2019). Copyright 2019 World Scientific Publishing. (b) Schematic diagram of the working principle of an active membrane-type AM controlled by a magnetic field and (c) metamaterial sample.[102] Reproduced with permission from Zhao *et al.*, J. Acoust. Soc. Am. **141**, 840–846 (2017). Copyright 2017 AIP Publishing LLC. (d) Active membrane-type AM controlled by an electric field and (e) the transmission coefficient and phase distribution under different external voltages.[106] Reproduced with permission from Xiao *et al.*, Appl. Phys. Lett. **106**, 091904 (2015). Copyright 2015 AIP Publishing LLC. (f) Transparent active membrane-type AM controlled by an electric field and (g) sound insulation performance measurement results.[108] Reproduced with permission from Rothemund *et al.*, Adv. Funct. Mater. **28**, 1800653 (2018). Copyright 2018 John Wiley and Sons. (h) Bilayer perforated active sound absorber controlled by an electric field and its (i) sound absorption performance measurement result.[109] Reproduced with permission from Lu *et al.*, J. Acoust. Soc. Am. **138**, EL236 (2015). Copyright 2015 AIP Publishing LLC.

the attraction of the magnet in the resonant cavity, allowing for a dynamic adjustment of the resonance frequency by modifying the membrane tension.[102] Although active magnetic metamaterials are light weight, generating and controlling the magnetic field often requires a relatively heavy device, making it challenging to meet the lightweight requirements during application. In addition to using piezoelectric materials and an external magnetic field, mechanical devices can also be used to achieve a tunable structural design. Davami et al. constructed a reconfigurable plate-type metamaterial that changed the configuration of the unit when exposed to external forces while also modifying the mechanical properties accordingly.[103] Langfeldt et al. designed a tunable bilayer membrane-type structure, with a mass disk on each membrane.[104] The cavity wall between the membrane layers produced a hole on the side through which compressed air at different volumes was injected to deform the membranes, obtaining effectively tunable parameters. Zhou et al. designed a flexible membrane-type periodic structure, in which the configuration of the unit changed when exposed to external forces, realizing the tunability of the elastic wave.[105] The mechanical control system used in active AMs is relatively simple. These structures exhibit a wide adjustable frequency range and easily designable components with significant load-bearing capacity. However, the real-time response performance of the mechanical device is poor, and it is suitable only for state switching. Therefore, it is challenging to adapt to applications where the operating frequency changes rapidly.

In addition to the methods mentioned above, tunable active metamaterials can also be designed by applying an external electric field. In 2015, Xiao et al. designed a membrane-type resonator structure, as shown in Fig. 15(d), that could actively adjust sound transmission. This structure consisted of a membrane-type metamaterial with a mass disk and an external mesh electrode that applied an electric field force to the membrane, changing its stiffness and shifting the resonance frequencies of the structure. Figure 15(e) shows that the frequency position of the transmission peak of the structures shifted accordingly after applying different external voltages. Therefore, the sound absorption frequency could be actively tuned since the resonant peak shifted at different external voltages.[107] Rothemund et al. used a transparent dielectric elastomer as an electrode to design a purely transparent, adjustable sound insulation metamaterial, as shown in Fig. 15(f). When alternating voltage was applied to control the phase shifts of the units, as shown in Fig. 15(g), broadband sound insulation with an average STL exceeding 15 dB was obtained in a broadband range of 200–1000 Hz.[108] Lu et al. arranged a rigid reflecting wall at the rear of a perforated actuator to form a resonant cavity, creating an active perforated sound-absorbing structure, as shown in Fig. 15(h).[109] They compared the sound absorption performance of an unperforated structure, a single-layer perforated structure, and a perforated bilayer structure, as shown in Fig. 15(i). Except for the multiple discrete sound absorption peaks produced by the unperforated structure, the sound absorption coefficients of the other frequencies were low. Although the amplitudes were slightly reduced at the original peaks after adding the perforating actuator, those at the original dips improved significantly while achieving excellent broadband sound absorption. In summary, many studies are available involving active metamaterials based on external electric fields. However, although the tunable characteristics can compensate for the shortcomings of

membrane tension, which is difficult to control quantitatively due to the use of soft membrane materials, guaranteeing the durability of structures is challenging. Moreover, the required driving voltage for many tasks is too high, which is inconvenient for large-scale applications. In addition to tunable sound insulation and sound absorption performance, active AMs can also be used for energy harvesting and various other applications.[129–131]

VI. CONCLUSIONS

In summary, since thin-walled metamaterials have been favored in the acoustic and vibration fields, they have attracted extensive attention for application in practical engineering. Specifically, thin-walled membrane-, plate-, and shell-type structures with deep subwavelength characteristics have significant value for engineering applications since they can meet light weight requirements. Extensive research in recent years has shown that different engineering applications have been realized in terms of sound insulation, sound absorption, and vibration reduction. It is expected that continuous development can help gradually realize a wide range of engineering applications within a few years. Although many advancements and breakthroughs have been made, significant challenges remain. The influence of lumped resonance in large-scale conditions significantly weakens the local resonance performance of metamaterial units, making it difficult to maintain the sound insulation performance realized by a small-sized structure. Therefore, it is preferable for large-sized applications to obtain strong low-frequency sound insulation in a specific frequency range via appropriate microstructure design rather than the entire frequency band.[117] In addition, considering application requirements, such as durability, it is ideal to use plate-type or shell-type structures rather than flexible membrane-type structures for microstructure design. Furthermore, it is necessary to balance the contradiction between the working bandwidth and the sample thickness to obtain low-frequency sound absorption below 500 Hz. The required thickness of a structure should be significant to entertain any hope for realizing broadband low-frequency sound absorption. However, if the structure thickness is low, only narrow-band absorption can be achieved. Due to the durability factor in membrane-type structures, perforated plates or shells are recommended for practical applications, which cooperate with resonant cavities or labyrinth channels to facilitate a synergetic coupling design. The relevant literature indicates that Helmholtz resonators are more commonly used for sound-absorbing AMs and metasurfaces. However, the size of a Helmholtz resonator is much larger than that of a thin-walled structure at a specific low frequency, which does not fulfill light-weight requirements. Thin-walled AMs present a disadvantage in that the sizes of the fabricated structures easily deviate from the design values. Consequently, the performance is sensitive to material parameters and fabrication technologies. With regard to vibration reduction, although the locally resonant periodic structures can effectively prevent vibration propagation, the mechanical properties of the original structure are destroyed, making them unsuitable in many conditions. Adding a vibration absorption unit is equivalent to improving and expanding the traditional dynamic vibration absorber, which is more suitable for engineering applications. In application conditions with more stringent

light weight requirements, the plate-type vibration-absorbing units are ideal, while a thicker, plate-type vibration absorption unit can be used in other application conditions.[132] Although membrane- and plate-type dampers can more easily achieve low-frequency vibration absorption than acoustic black hole structures, their working bandwidths are not as wide.

Thin-walled structures are significantly important from a research perspective due to their unique advantages and application value. By combining them with current development tendencies in the acoustic and EM fields, it is conceivable that future research trends may include, but may not be limited to, the following: (1) focusing on lightweight thin-walled structures, such as topological acoustics and non-Hermitian acoustics, to achieve unique physical and mechanical properties.[21] (2) Synthesizing related theories from both a design and a manufacturing perspective to develop material-structure-function-integrated design and manufacturing schemes. (3) Developing new design methods, such as synergetic coupling techniques, and fully utilizing the synergistic coupling relationship between different components, such as sub-cells and multi-cells, to design functional devices with more compact structures for performance enhancement.[42,50] (4) Integrating multiple physical and mechanical functions into one set of structures to develop a multi-objective design for creating highly integrated multi-functional devices. (5) Introducing traditional mechanical and structural design methods, such as topology optimization and bionic designs, to construct microstructures with enhanced acoustic performance.[133]

ACKNOWLEDGMENTS

DATA AVAILABILITY

The data that support the findings of this study are available from the corresponding author upon reasonable request.

REFERENCES

[1]G. Davixs, Aust. For. **41**, 153–159 (1978).
[2]C. Morrow, J. Acoust. Soc. Am. **55**, 695–699 (1974).
[3]E. Eijkman and A. Vendrik, J. Acoust. Soc. Am. **32**, 1134–1139 (1960).
[4]W. Carey and R. Wagstaff, J. Acoust. Soc. Am. **80**, 1523–1526 (1986).
[5]B. Berglund, P. Hassmén, and R. Job, J. Acoust. Soc. Am. **99**, 2985–3002 (1996).
[6]K. Mulholland and R. Lyon, J. Acoust. Soc. Am. **54**, 867–878 (1973).
[7]M. Rettinger, J. Acoust. Soc. Am. **56**, 1511–1514 (1974).
[8]S. Ljunggren, J. Acoust. Soc. Am. **89**, 2324–2337 (1991).
[9]S. Ljunggren, J. Acoust. Soc. Am. **89**, 2338–2345 (1991).
[10]Z. Liu, X. Zhang, Y. Mao, Y. Zhu, Z. Yang, C. Chan, and P. Sheng, Science **289**, 1734–1736 (2000).
[11]J. Li and C. Chan, Phys. Rev. E **70**, 055602 (2004).
[12]N. Fang, D. Xi, J. Xu, M. Ambati, W. Srituravanich, C. Sun, and X. Zhang, Nat. Mater. **5**, 452–456 (2006).
[13]Y. Ding, Z. Liu, C. Qiu, and J. Shi, Phys. Rev. Lett. **99**, 093904 (2007).
[14]G. Ma and P. Sheng, Sci. Adv. **2**, e1501595 (2016).
[15]S. Cummer, J. Christensen, and A. Alù, Nat. Rev. Mater. **1**, 16001 (2016).
[16]T. Huang, C. Shen, and Y. Jing, J. Acoust. Soc. Am. **139**, 3240–3250 (2016).
[17]R. Zhu, X. Liu, G. Hu, F. Yuan, and G. Huang, Int. J. Smart Nano Mater. **6**, 14–40 (2015).
[18]Y. Wu, M. Yang, and P. Sheng, J. Appl. Phys. **123**, 090901 (2018).
[19]X. Zhang, Z. Qu, and H. Wang, iScience **23**, 101110 (2020).
[20]B. Assouar, B. Liang, Y. Wu, Y. Li, J. Cheng, and Y. Jing, Nat. Rev. Mater. **3**, 460–472 (2018).
[21]G. Ma, M. Xiao, and C. Chan, Nat. Rev. Phys. **1**, 281–294 (2019).
[22]K. Bertoldi, V. Vitelli, J. Christensen, and M. van Hecke, Nat. Rev. Mater. **2**, 17066 (2017).
[23]Z. Yang, J. Mei, M. Yang, N. Chan, and P. Sheng, Phys. Rev. Lett. **101**, 204301 (2008).
[24]C. Naify, C. Chang, G. McKnight, and S. Nutt, J. Appl. Phys. **108**, 114905 (2010).
[25]Y. Zhang, J. Wen, Y. Xiao, X. Wen, and J. Wang, Phys. Lett. A **376**, 1489–1494 (2012).
[26]C. Naify, C. Chang, G. McKnight, and S. Nutt, J. Appl. Phys. **110**, 124903 (2011).
[27]M. Oudich, X. Zhou, and M. Badreddine Assouzar, J. Appl. Phys. **116**, 193509 (2014).
[28]Z. Lu, X. Yu, S. Lau, B. Khoo, and F. Cui, Appl. Acoust. **157**, 107003 (2020).
[29]F. Ma, J. Wu, M. Huang, W. Zhang, and S. Zhang, J. Phys. D: Appl. Phys. **48**, 175105 (2015).
[30]N. Sui, X. Yan, T. Huang, J. Xu, F. Yuan, and Y. Jing, Appl. Phys. Lett. **106**, 171905 (2015).
[31]A. Peiffer, M. Grünewald, and P. Lempereur, Appl. Phys. Lett. **107**, 216101 (2015).
[32]F. Ma, Y. Xu, and J. Wu, Sci. Rep. **9**, 8076 (2019).
[33]Z. Yang, H. Dai, N. Chan, G. Ma, and P. Sheng, Appl. Phys. Lett. **96**, 041906 (2010).
[34]F. Ma, J. Wu, and M. Huang, J.Phys. D: Appl. Phys. **48**, 465305 (2015).
[35]L. Fan, Z. Chen, S. Zhang, J. Ding, X. Li, and H. Zhang, Appl. Phys. Lett. **106**, 151908 (2015).
[36]J. Chen, Y. Chen, H. Chen, and Y. Yeh, Mater. Res. Express **3**, 105801 (2016).
[37]F. Ma, M. Huang, Y. Xu, and J. Wu, J. Appl. Phys. **123**, 035104 (2018).
[38]L. Ang, Y. Koh, and H. Lee, Appl. Phys. Lett. **112**, 051903 (2018).
[39]C. Naify, C. Chang, G. McKnight, F. Scheulen, and S. Nutt, J. Appl. Phys. **109**, 104902 (2011).
[40]Y. Zhang, J. Wen, H. Zhao, D. Yu, L. Cai, and X. Wen, J. Appl. Phys. **114**, 063515 (2013).
[41]F. Ma, M. Huang, and J. Wu, J. Appl. Phys. **121**, 015102 (2017).
[42]F. Ma, M. Huang, and J. Wu, J. Appl. Phys. **122**, 215102 (2017).
[43]X. Wang, Y. Chen, G. Zhou, T. Chen, and F. Ma, J. Sound Vib. **459**, 114867 (2019).
[44]L. Ang, Y. Koh, and H. Lee, Appl. Acoust. **149**, 156–170 (2019).
[45]J. Mei, G. Ma, M. Yang, Z. Yang, W. Wen, and P. Sheng, Nat. Commun. **3**, 756 (2012).
[46]Y. Chen, G. Huang, X. Zhou, G. Hu, and C. Sun, J. Acoust. Soc. Am. **136**, 969–979 (2014).
[47]Y. Chen, G. Huang, X. Zhou, G. Hu, and C. Sun, J. Acoust. Soc. Am. **136**, 2926–2934 (2014).
[48]C. Liu, J. Wu, K. Lu, Z. Zhao, and Z. Huang, Appl. Acoust. **148**, 1–8 (2019).
[49]G. Ma, M. Yang, S. Xiao, Z. Yang, and P. Sheng, Nat. Mater. **13**, 873–878 (2014).
[50]F. Ma, M. Huang, Y. Xu, and J. Wu, Sci. Rep. **8**, 5906 (2018).
[51]X. Gai, X. Li, B. Zhang, T. Xing, J. Zhao, and Z. Ma, Appl. Acoust. **110**, 241–247 (2016).
[52]Y. Tang, F. Xin, L. X. Huang, and T. Lu, Europhys. Lett. **118**, 44002 (2017).
[53]X. Gai, T. Xing, X. Li, B. Zhang, Z. Cai, and F. Wang, Appl. Acoust. **137**, 98–107 (2018).
[54]X. Peng, J. Ji, and Y. Jing, J. Acoust. Soc. Am. **144**, EL255 (2018).
[55]H. Kim, P. Ma, B. Kim, S. Kim, and S. Lee, J. Sound Vib. **460**, 114884 (2019).
[56]F. Ma, J. Chen, and J. Wu, J. Mater. Chem. C **7**, 5131 (2019).
[57]C. Maury and T. Bravo, J. Sound Vib. **478**, 115356 (2020).

[58] J. Hsu and T. Wu, Appl. Phys. Lett. **90**, 201904 (2007).

[59] Y. Pennec, B. Djafari-Rouhani, H. Larabi, J. Vasseur, and A. Hladky-Hennion, Phys. Rev. B **78**, 104105 (2008).

[60] T. Wu, Z. Huang, T. Tsai, and T. Wu, Appl. Phys. Lett. **93**, 111902 (2008).

[61] T. Wu, T. Wu, and J. Hsu, Phys. Rev. B **79**, 104306 (2009).

[62] M. Oudich, Y. Li, B. M. Assouar, and Z. Hou, New J. Phys. **12**, 083049 (2010).

[63] Y. El Hassouani, C. Li, Y. Pennec, E. El Boudouti, H. Larabi, A. Akjouj, O. Bou Matar, V. Laude, N. Papanikolaou, A. Martinez, and B. Djafari Rouhani, Phys. Rev. B **82**, 155405 (2010).

[64] M. Oudich, M. Senesi, M. Assouar, M. Ruzenne, J. Sun, B. Vincent, Z. Hou, and T. Wu, Phys. Rev. B **84**, 165136 (2011).

[65] J. C. Hsu, J. Phys. D: Appl. Phys. **44**, 055401 (2011).

[66] S. Zhang, J. Wu, and Z. Hu, J. Appl. Phys. **113**, 163511 (2013).

[67] M. Oudich, B. Djafari-Rouhani, Y. Pennec, M. Assouar, and B. Bonello, J. Appl. Phys. **116**, 184504 (2014).

[68] D. Beli, J. Arruda, and M. Ruzzene, Int. J. Solids Struct. **139–140**, 105–120 (2018).

[69] J. Shi, C. Liu, and Y. Lai, New J. Phys. **20**, 103043 (2018).

[70] F. Ma, Y. Xu, and J. Wu, Appl. Phys. Express **12**, 074004 (2019).

[71] R. Zhu, X. Liu, G. Hu, C. Sun, and G. Huang, J. Sound Vib. **333**, 2759–2773 (2014).

[72] M. Nouh, O. Aldraihem, and A. Baz, J. Sound Vib. **341**, 53–73 (2015).

[73] A. Pelat, F. Gautier, S. Conlon, and F. Semperlotti, J. Sound Vib. **476**, 115316 (2020).

[74] Y. Wu, Y. Lai, and Z. Zhang, Phys. Rev. Lett. **107**, 105506 (2011).

[75] Y. Lai, Y. Wu, P. Sheng, and Z. Zhang, Nat. Mater. **10**, 620–624 (2011).

[76] Z. Chang and G. Hu, Appl. Phys. Lett. **101**, 054102 (2012).

[77] J. Zhu, Y. Liu, Z. Liang, T. Chen, and J. Li, Phys. Rev. Lett. **121**, 234301 (2018).

[78] X. Chen, L. Cai, and J. Wen, Chin. Phys. B **27**, 057803 (2018).

[79] P. Gao, A. Climente, J. Sanchez-Dehesa, and L. Wu, J. Sound Vib. **444**, 108–126 (2019).

[80] H. Peng and P. Frank Pai, Int. J. Mech. Sci. **89**, 350–361 (2014).

[81] T. Wang, M. Sheng, Z. Guo, and Q. Qin, Appl. Acoust. **114**, 118–124 (2016).

[82] L. Sun, K. Au-Yeung, M. Yang, S. Tang, Z. Yang, and P. Sheng, AIP Adv. **6**, 085212 (2016).

[83] K. Matlack, A. Bauhofer, S. Krödel, A. Palermo, and C. Daraio, Proc. Natl. Acad. Sci. U.S.A. **113**, 8386–8390 (2016).

[84] S. Yeh and R. Harne, Smart Mater. Struct. **29**, 085010 (2020).

[85] Z. Zhai, H. Chen, C. Ding, L. Li, F. Shen, C. Luo, and X. Zhao, J. Phys. D: Appl. Phys. **49**, 225302 (2016).

[86] F. Ma, Y. Xu, and J. Wu, Appl. Phys. Express **12**, 054003 (2019).

[87] X. Wang, D. Mao, and Y. Li, Sci. Rep. **7**, 11604 (2017).

[88] A. Colombi, P. Roux, S. Guenneau, and M. Rupin, J. Acoust Soc. Am. **137**, 1783–1789 (2015).

[89] M. Lee and Y. Kim, Sci. Rep. **6**, 20731 (2016).

[90] Y. Xu, L. Cao, and Z. Yang, J. Sound Vib. **454**, 51–62 (2019).

[91] S. Yuan, A. Chen, and Y. Wang, J. Sound Vib. **470**, 115168 (2020).

[92] J. Zhang, X. Zhang, F. Xu, X. Ding, M. Deng, N. Hu, and C. Zhang, J. Sound Vib. **481**, 115440 (2020).

[93] V. Fokin, M. Ambati, C. Sun, and X. Zhang, Phys. Rev. B **76**, 144302 (2007).

[94] M. Yang, G. Ma, Z. Yang, and P. Sheng, Phys. Rev. Lett. **110**, 134301 (2013).

[95] P. Li, S. Yao, X. Zhou, G. Huang, and G. Hu, J. Acoust. Soc. Am. **135**, 1844–1852 (2014).

[96] Y. Xu, J. Wu, Y. Cai, and F. Ma, J. Phys. D: Appl. Phys. **52**, 405301 (2019).

[97] S. Kumar and H. Pueh Lee, Int. J. Appl. Mech. **11**, 1950081 (2019).

[98] Y. Wang, Y. Wang, B. Wu, W. Chen, and Y. Wang, Appl. Mech. Rev. **72**, 040801 (2020).

[99] B. Popa, L. Zigoneanu, and S. Cummer, Phys. Rev. B **88**, 024303 (2013).

[100] X. Zhang, F. Chen, Z. Chen, and G. Wang, J. Acoust. Soc. Am. **144**, 3514–3524 (2018).

[101] X. Chen, X. Xu, S. Ai, H. Chen, Y. Pei, and X. Zhou, Appl. Phys. Lett. **105**, 71913 (2014).

[102] J. Zhao, X. Li, Y. Wang, W. Wang, B. Zhang, and X. Gai, J. Acoust. Soc. Am. **141**, 840–846 (2017).

[103] K. Davami, L. Zhao, E. Lu, J. Cortes, C. Lin, D. Lilley, P. Purohit, and I. Bargatin, Nat. Commun. **6**, 10019 (2015).

[104] F. Langfeldt, J. Riecken, W. Gleine, and O. von Estorff, J. Sound Vib. **373**, 1–18 (2016).

[105] W. Zhou, B. Wu, Muhammad, Q. Du, G. Huang, C. Lu, and W. Q. Chen, J. Appl. Phys. **123**, 165304 (2018).

[106] S. Xiao, G. Ma, Y. Li, Z. Yang, and P. Sheng, Appl. Phys. Lett. **106**, 091904 (2015).

[107] Z. Lu, Y. Cui, M. Debiasi, and Z. Zhao, Acta Acust. United Ac. **101**, 863–866 (2015).

[108] P. Rothemund, X. Morelle, K. Jia, G. Whitesides, and Z. Suo, Adv. Funct. Mater. **28**, 1800653 (2018).

[109] Z. Lu, H. Godaba, Y. Cui, C. Foo, M. Debiasi, and J. Zhu, J. Acoust. Soc. Am. **138**, EL236 (2015).

[110] H. Cohen and G. Handelman, J. Acoust. Soc. Am. **29**, 229–233 (1957).

[111] N. Romilly, J. Acoust. Soc. Am. **36**, 1104–1109 (1964).

[112] G. Kriegsmann, A. Norris, and E. Reiss, J. Acoust. Soc. Am. **75**, 685–694 (1984).

[113] D. Ahluwalia, G. Kriegsmann, and E. Reiss, J. Acoust. Soc. Am. **78**, 682–687 (1985).

[114] A. Norris and D. Rebinsky, J. Acoust. Soc. Am. **97**, 2063–2073 (1995).

[115] M. Amabili, M. Pellegrini, F. Righi, and F. Vinci, J. Sound Vib. **295**, 1–12 (2006).

[116] K. Lu, J. Wu, D. Guan, N. Gao, and L. Jing, AIP Adv. **6**, 025116 (2016).

[117] C. Droz, O. Robin, M. Ichchou, and N. Atalla, J. Acoust. Soc. Am. **145**, EL72 (2019).

[118] F. Langfeldt and W. Gleine, J. Sound Vib. **453**, 65–86 (2019).

[119] C. Liu, J. Wu, X. Chen, and F. Ma, J. Phys. D: Appl. Phys. **52**, 105302 (2019).

[120] C. Liu, J. Wu, F. Ma, X. Chen, and Z. Yang, Appl. Phys. Express **12**, 084002 (2019).

[121] C. Rui Liu, J. Hui Wu, Z. Yang, and F. Ma, Compos. Struct. **246**, 112366 (2020).

[122] H. Zhao, Y. Wang, D. Yu, H. Yang, J. Zhong, F. Wu, and J. Wen, Compos. Struct. **239**, 111978 (2020).

[123] S. Huang, Z. Zhou, D. Li, T. Liu, X. Wang, J. Zhu, and Y. Li, Sci. Bull. **65**, 373–379 (2020).

[124] H. Liu, J. Wu, B. Li, Y. Lei, and F. Ma, J. Phys. D: Appl. Phys. **53**, 495301 (2020).

[125] F. Ma, Y. Cai, and J. Wu, J. Phys. D: Appl. Phys. **54**, 055303 (2021).

[126] Y. Chen, G. Huang, and C. Sun, J. Vib. Acoust. **136**, 061008 (2014).

[127] Y. Chen, J. Hu, and G. Huang, J. Intel. Mat. Syst. Str. **27**, 1337–1347 (2016).

[128] Y. Chen, G. Hu, and G. Huang, Smart Mater. Struct. **25**, 105036 (2016).

[129] H. Nguyen, R. Zhu, J. Chen, S. Tracy, and G. Huang, Smart Mater. Struct. **27**, 055010 (2018).

[130] Y. Chen, X. Li, H. Nassar, G. Hu, and G. Huang, Smart Mater. Struct. **27**, 115011 (2018).

[131] Y. Chen, X. Li, G. Hu, M. R. Haberman, and G. Huang, Nat. Commun. **11**, 3681 (2020).

[132] F. Ma, J. Wu, M. Huang, G. Fu, and C. Bai, Appl. Phys. Lett. **105**, 213702 (2014).

[133] Y. Cai, J. Hui Wu, Y. Xu, and F. Ma, Compos. Struct. **262**, 113351 (2021).